GEOPHYSICAL SURVEY FOR CHARACTERIZING THE HYDRO-GEOLOGIC REGIME OF THE PUU ANAHULU AREA OF NORTH KONA, ISLAND OF HAWAII

BLACKHAWK GEOSCIENCES, INC.

GEOPHYSICAL SURVEY FOR CHARACTERIZING THE HYDROGEOLOGIC REGIME OF THE PUU ANAHULU AREA OF NORTH KONA ISLAND OF HAWAII

Prepared For:

State of Hawaii
Department of Land and Natural Resources
Division of Water Resource Management
Kalanimoku Bldg., Room 227
1151 Punchbowl Street
Honolulu, HI 96809

Prepared By:

Blackhawk Geosciences, Inc.
17301 West Colfax Ave., Suite 170
Golden, CO 80401

(BGI Project #91052)

December 3, 1991

Table of Contents

1.0 INTRODUCTION

This report contains the results of time domain electromagnetic (TDEM) geophysical surveys for ground water resource evaluation of the Puu Anahulu area of North Kona on the Island of Hawaii. The survey was performed by Blackhawk Geosciences, Inc. (BGI) for the Division of Water Resource Management, State of Hawaii, from October 29 to November 3, 1991.

The main objective of the geophysical survey was to characterize the hydrologic regime near Puu Anahulu. The concept for using geophysical surveys for ground water evaluations can be understood using the generalized hydrogeologic cross section shown in Figure 1-1. In the Hawaiian islands, the volcanic rocks are generally highly permeable and rain water rapidly percolates into the ground and migrates downward to the water table. Fresh ground water in island settings is generally found in two environments:

1. Dike-confined waters. Intrusive dikes originating from a magma source below can form ground water dams, and behind these natural dams significant quantities of ground water can be stored.

2. Basal fresh water. The high permeability of the volcanic rocks allows sea water to enter freely under the island, and a delicate balance is reached where a lens of fresh water floats on sea water. In cases where hydrostatic equilibrium exists, the Ghyben-Herzberg relation states that for every foot of fresh water head above sea level there will be 40 ft of fresh water below sea level.

The basal mode water resource was the main focus in the investigations for the State of Hawaii.

Because the electrical resistivity of rock formations is highly dependent upon the salinity of ground water, electrical surface geophysical techniques can map the depth to salt water, and the thickness of the fresh water lens can then be estimated using the Ghyben-Herzberg principle. The impetus for using geophysics is that the cost of a geophysical sounding is about one-thousandth the cost of completing a well at elevations above 1,000 ft. Geophysical surveys, combined with other hydrogeologic information, are used to provide optimum locations for well placement and well completion depths. The specific geophysical method employed was time domain electromagnetic (TDEM) soundings. This method was selected because it has proven effective in prior surveys in similar settings in Hawaii.

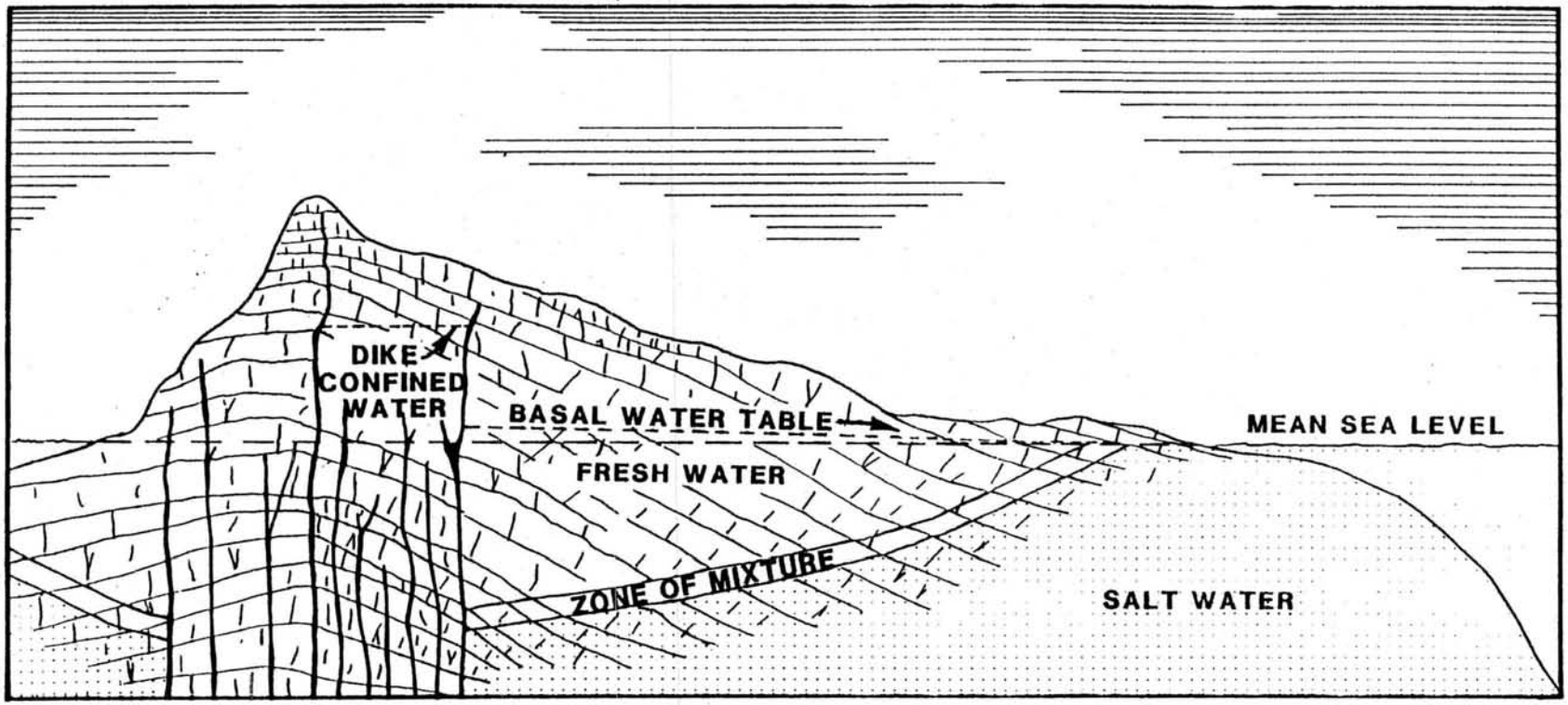

BLACKHAWK GEOSCIENCES, INC.

SCHEMATIC HYDRO-GEOLOGIC CROSS SECTION

DIVISION OF WATER RESOURCES MGMT.
STATE OF HAWAII

PROJECT NO: 81054 FIGURE 1-1

2.0 LOGISTICS AND DATA ACQUISITION PROCEDURES

The TDEM survey was performed by a three man crew consisting of two BGI geophysicists and one local field helper. The locations of the sounding sites were determined during consultation with State personnel and their consulting hydrologist. Due to the remoteness of the project area, no jeep roads or trails were available for access. Therefore, helicopter support was supplied by the Client for the duration of the field survey. At the start of the survey a base control point (BCP) was established on the east corner of sounding 1. The BCP was surveyed in by compass and hip-chain on bearing with the road west of Puu Hinai, and to the north edge of the Kaniku lava flow. The survey line numbers and loop locations are shown on Figure 2-1.

During the five days of field work, a total of 10 sounding measurements were acquired over the area of interest. As the survey progressed the location and number of soundings changed at the request of the consulting hydrologist, to include only measurements between approximately the 1,400 ft and 1,700 ft elevation level. From the BCP, bearings of $N40^0W$ and $S50^0W$ were used throughout the survey area to layout transmitter loops and when measuring from loop-to-loop and from line-to-line. Elevations of sounding centers were measured with a handheld barometric altimeter in the field and checked periodically against the helicopter altimeter during each day to maintain reliable ($\pm$ 20 ft) elevation readings. A daily log of field activities during the survey is given in Table 2-1. Transmitter loop sizes varied from 1,000 ft by 1,000 ft to 1,200 ft by 1,200 ft in the study area according to depth of investigation needed and the logistics of accomplishing the sounding measurement.

2.1 PROCEDURES

The Geonics EM-37 TDEM system was utilized on this survey. The system basically consists of a transmitter and a receiver. The transmitter loop is constructed of 10 to 12 gauge insulated copper wire. The wire is laid on the ground surface in a square loop varying in size, depending upon the required depth of investigation (larger loop sizes for deeper measurement). A transmitter and motor generator are connected into the non-grounded loop at one corner. A time-varying current is pulsed through the wire at two different base frequencies. The TDEM receiver measures and records the decay of the vertical magnetic field through a receiver coil placed at the center of the non-grounded transmitter loop. Receiver coils with effective areas of 100 m^2 and 1,000 m^2 were utilized at base frequencies of 3 Hz and 30 Hz. During data acquisition numerous transient decays are collected with the receiver for each sounding. Readings were acquired at several receiver gains with opposite receiver polarities for each sounding location. The readings were stored

in a DAS-54 solid state data logger, and were nightly transferred to a personal computer for processing. A technical note is given in Appendix A which describes and illustrates the principles of TDEM.

Table 2-1. Daily log of field activities

Date (1991)	Activity
October 27	Demobilize from other Pacific jobs to Kailua-Kona, HI in conjunction with other surveys.
October 28	One-half day of mobilization, clear equipment through customs.
October 29	Perform reconnaissance of sounding site 1, and establish base control point (BCP) on east corner. Transport TDEM equipment and crew by helicopter to east corner of sounding 1. Acquire measurement of soundings 1 and 2.
October 30	Measurement of soundings 3 and 4.
October 31	Measurement of soundings 5 and 6.
November 2	Measurement of soundings 7 and 8.
November 3	Measurement of soundings 9 and 10.
November 4-5	Demobilization of equipment and BGI personnel from Kailua-Kona, HI to Golden, CO.
	(October 28 and November 1 are work at other Hawaii locations)

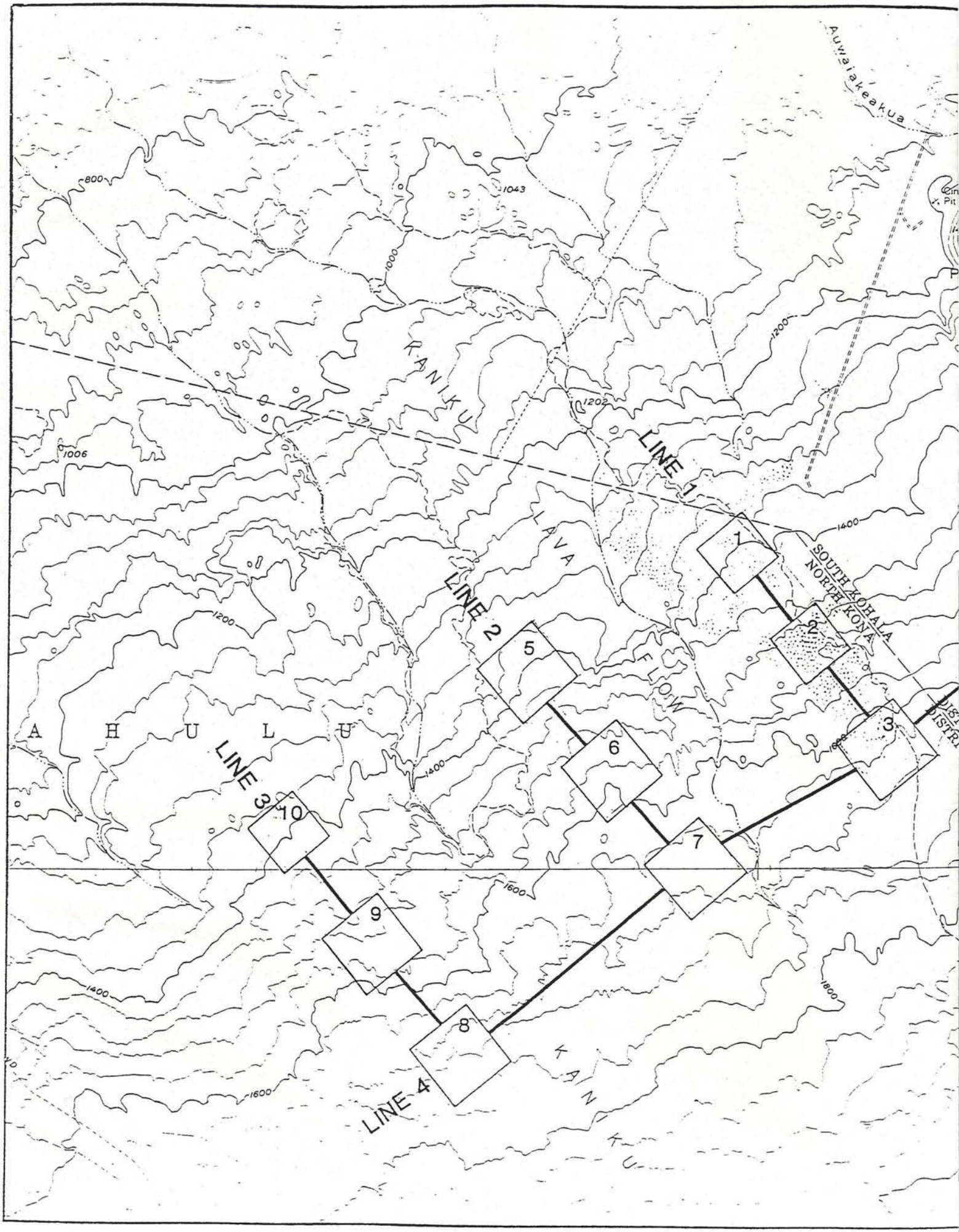
Auwaiakeakua
800
1043
1000
1200
1202
1006
KANIKU
LAVA
FLOW
LINE 1
LINE 2
LINE 3
LINE 4
1400
1600
1800
AHULUU
SOUTH KOHALA
NORTH KONA
1
2
3
5
6
7
8
9
10
KANKU

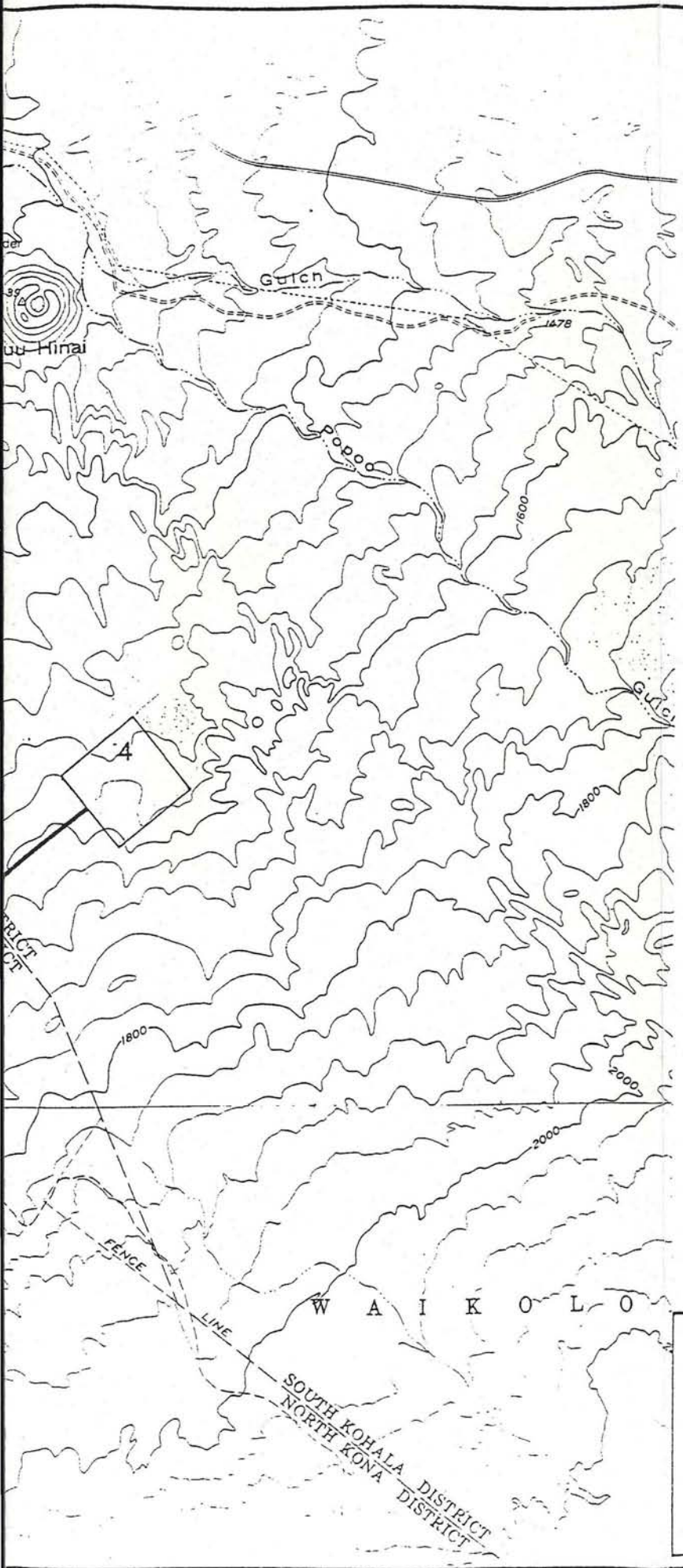

4 Sounding Location and Number

Geoelectric Cross Section

PUU HINAI AND PUU ANAHULU QUADRANGLES

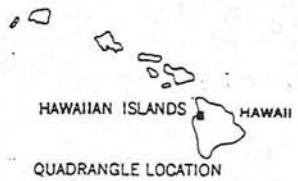

QUADRANGLE LOCATION

0 2000 4000 Feet

BLACKHAWK GEOSCIENCES, INC.

TIME DOMAIN EM SURVEY LOCATION MAP

DIVISION OF WATER RESOURCES MGMT.
STATE OF HAWAII

PROJECT NO: 91054 Figure 2-1

3.0 DATA PROCESSING

The field data acquired each day was transferred from the DAS-54 data logger to a personal computer. The data for each sounding location is edited and combined (both 3 Hz and 30 Hz frequencies) to produce a transient decay curve. This decay curve is transformed into an apparent resistivity curve, which is entered into an Automatic Ridge Regression Transient Inversion Program (ARRTI). From the apparent resistivity curve a one-dimensional model of resistivities and thicknesses is calculated.

The inversion program requires an initial estimate of the geoelectric section, including the number of layers, and the resistivities and thicknesses of each of the layers. The program then adjusts these parameters so that the model curve converges to best fit the curve formed by the field data set. The inversion program does not change the total number of layers within the model, but allows all other parameters to float freely.

An example data set is given in Figures 3-1 and 3-2 for sounding WAIK1 (sounding number 1). Figure 3-1 shows the measured data points (in terms of apparent resistivity) superimposed on a solid line. The solid line represents the computed behavior of the true resistivity layering shown on the right. Thus, the section is interpreted to consist of two layers, - the first layer has a thickness of 527 m (1,729 ft) with a resistivity of 3,799 ohm-m, and the resistivity of the second layer is 2.8 ohm-m. Figure 3-2 lists model and survey parameters, and in column 4 the error between measured and computed data in each time gate.

The apparent resistivity curves and data sheets for all soundings are contained in Appendix B.

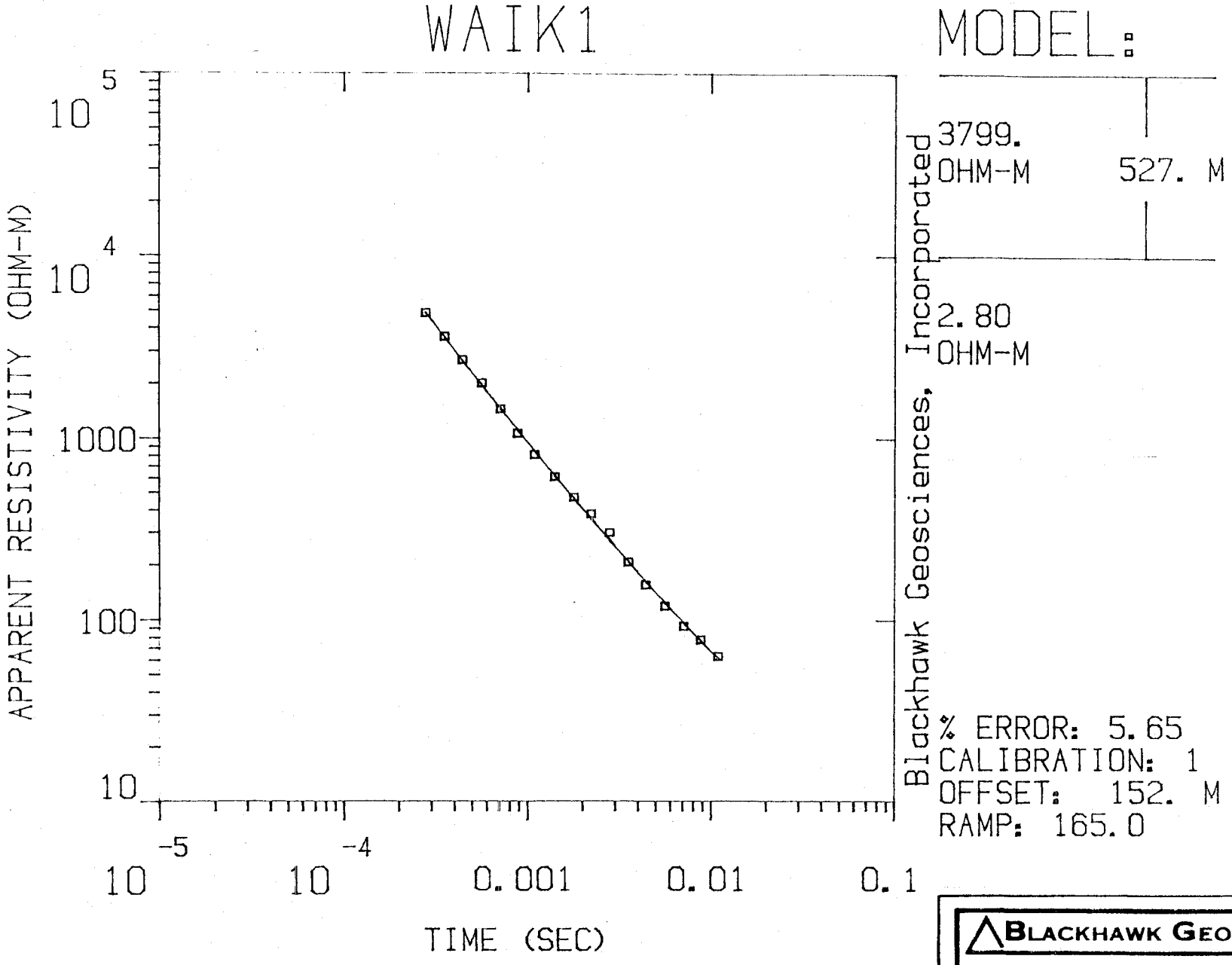

BLACKHAWK GEOSCIENCES, INC.

EXAMPLE DATA SET
SOUNDING WAIK1
DIVISION OF WATER RESOURCE MGMT.
STATE OF HAWAII

PROJECTNO: 91054 Figure 3-1

MODEL: 2 LAYERS

RESISTIVITY (OHM-M)	THICKNESS (M)	ELEVATION (M)	ELEVATION (FEET)	CONDUCTANCE (S) LAYER	CONDUCTANCE (S) TOTAL
		426.7	1400.0		
3799.13	527.1	-100.3	-329.2	0.1	0.1
2.80					

	TIMES	DATA	CALC	% ERROR	STD ERR
1	2.80E-04	4.83E+03	4.86E+03	-0.654	
2	3.55E-04	3.60E+03	3.56E+03	1.050	
3	4.43E-04	2.69E+03	2.67E+03	0.837	
4	5.64E-04	2.00E+03	1.96E+03	2.250	
5	7.13E-04	1.44E+03	1.45E+03	-0.730	
6	8.81E-04	1.06E+03	1.11E+03	-4.274	
7	1.10E-03	8.14E+02	8.49E+02	-4.062	
8	1.41E-03	6.13E+02	6.22E+02	-1.346	
9	1.80E-03	4.72E+02	4.64E+02	1.701	
10	2.22E-03	3.81E+02	3.60E+02	5.959	
11	2.80E-03	3.01E+02	2.74E+02	9.748	
12	3.55E-03	2.08E+02	2.09E+02	-0.474	
13	4.43E-03	1.56E+02	1.62E+02	-3.839	
14	5.64E-03	1.19E+02	1.24E+02	-3.962	
15	7.13E-03	9.24E+01	9.65E+01	-4.237	
16	8.81E-03	7.81E+01	7.70E+01	1.406	
17	1.10E-02	6.32E+01	6.15E+01	2.708	

R: 152. X: 0. Y: 152. DL: 305. REQ: 169. CF: 1.0000
TDHZ ARRAY, 17 DATA POINTS, RAMP: 165.0 MICROSEC, DATA: WAIK1
2910 1111 1111 Z OPR XTL L 6 10+1000
Ch.21 = 0.165 Ch.22 = 0.89 Ch.23 = 15 Ch.24 = 9
RMS LOG ERROR: 2.39E-02, ANTILOG YIELDS 5.6524 %
LATE TIME PARAMETERS

* Blackhawk Geosciences, Incorporated *

PARAMETER RESOLUTION MATRIX:
"F" MEANS FIXED PARAMETER
P 1 0.97
F 2 0.00 0.00
T 1 0.00 0.00 1.00
P 1 F 2 T 1

BLACKHAWK GEOSCIENCES, INC.

EXAMPLE DATA SET
SOUNDING WAIK1
DIVISION OF WATER RESOURCES MGMT.
STATE OF HAWAII

PROJECT NO: 91054 Figure 3-2

4.0 INTERPRETATION RESULTS

4.1 GENERAL

The objectives of the geophysical survey for the State of Hawaii were to interpret from the individual TDEM soundings the resistivity layering as a function of depth. Also, to infer from the resistivity information the depth to salt water, and the thickness of the basal fresh water lens. The TDEM soundings were purposely acquired along traverse lines from about the 1,400 ft to 1,700 ft elevation level. The results of the individual soundings were used to construct geoelectric cross sections through several transects. From the 10 soundings taken on the area of interest, four geoelectric cross sections were constructed to display the interpreted data set. Figure 2-1 shows the locations of the soundings and the geoelectric cross sections.

Using available knowledge about the relation between resistivity values and local hydrogeology, geologic and geohydrologic information was inferred from geoelectric cross sections. The characteristic ranges of resistivities expected for local geohydrologic units in the survey area are shown in Figure 4-1. The resistivity range for ash flows, weathered volcanics or intrusives overlaps both the lower range of the dry unweathered or fresh/brackish water saturated volcanics and the upper range for salt water saturated volcanics. In many cases the geohydrologic units can be separated by their relative depth of occurrence in the section.

In the TDEM interpretation, where a very conductive layer (< 5 ohm-m) is detected below sea level, this layer is expected to be caused by salt water saturated volcanics. For this survey a fixed 2.8 ohm-m resistivity value was used to represent the resistivity of the salt water saturated layer. The validity of using this resistivity value for salt water saturated volcanics was confirmed by a previous TDEM survey in the Waikoloa area to the north. Static water levels (heads) can subsequently be calculated from these soundings by using the Ghyben-Herzberg principle. This principle states that under conditions of static equilibrium, for every foot of fresh water above sea level there will be about forty feet of fresh water below sea level. An illustration of the Ghyben-Herzberg principle is given in Figure 4-2. This principle, however, assumes static equilibrium and may not apply to TDEM sounding data in close proximity to ground water damming structures (i.e., dikes, rifts, etc.).

TDEM soundings in areas where ground water has been shown to be dike-confined, typically show high resistivity (greater than 100 ohm-m) layers to the exploration depth of the TDEM system (typically -800 ft below sea level). In other words, no sea water saturated formations are interpreted within the entire

section. Within the structure controlled areas which separate the basal mode and dike-confined areas, TDEM data often exhibit intermediate resistivity values (10 to 100 ohm-m) that may occur both above and below sea level. In cases where intermediate resistivities occur well below sea level (-300 to -500 ft) it is generally not possible to determine the exact origin and nature of the subsurface conditions influencing the formation resistivities. The data taken in these areas may be distorted or influenced by the nearby structures and may not be diagnostic of true resistivity layering. This is due to the large subsurface areas that are averaged below a large transmitter loop (1,500 ft by 1,500 ft) and the limitation of present 1-D interpretations for TDEM data.

4.2 GEOELECTRIC CROSS SECTIONS

The results of the 10 TDEM sounding interpretations are presented as four geoelectric cross sections and are shown in Figures 4-3 and 4-4. Layers with similar resistivities have been linked together in the geoelectric sections.

Lines 1 and 2

The geoelectric cross sections for Lines 1 and 2 are both presented as northwest to southeast transects in Figure 4-3. Similar two-layer sequences are interpreted in the geoelectric cross sections for Lines 1 and 2. The upper layer of these two geoelectric cross sections exhibit high resistivities ranging from 2,857 ohm-m at sounding 3 to greater than 9,000 ohm-m at sounding 5 and are interpreted to represent unweathered volcanics. Below sea level, in both cross sections, this resistive layer is expected to be saturated with fresh/brackish water. The lower layer in both lines has been fixed to a 2.8 ohm-m resistivity and is interpreted to represent salt water saturated volcanics. The approximate thickness of the fresh/brackish water lens for these soundings was found to vary between 329 ft at sounding 1 to 430 ft beneath sounding 2.

Lines 3 and 4

In Figure 4-4 the geoelectric cross section for Lines 3 and 4 are displayed. The soundings were interpreted with either a two or three layer geoelectric section. The upper layer in both cross sections exhibits high resistivity values ranging from 1,312 ohm-m to greater than 6,000 ohm-m. This upper layer at soundings 7, 3 and 4 is interpreted to represent dry unweathered volcanics above sea level, and where it occurs below sea level, it is expected to be saturated with fresh/brackish basal mode water. The lower layer of Line 3 (and sounding 8 on Line 4) exhibits intermediate resistivity values ranging from 9.2 ohm-m to 71 ohm-m. This lower layer may be caused by changes in

lithology (ash flows, weathered volcanics), changes in water quality or geologic structure.

Beneath soundings 3, 4 and 7 of Line 4 where the lower layer is interpreted to represent salt water saturated volcanics, the approximate thickness of the fresh/brackish water lens can be estimated from these soundings and it was found to vary from 344 ft at sounding 4 to 396 ft at sounding 7. Because of the rapid resistivity contrasts between soundings 7 and 8 (2.8 ohm-m to 71 ohm-m) lateral changes are expected to occur between the two soundings and a geologic structure is inferred.

4.3 HYDROGEOLOGIC INTERPRETATIONS

Table 4-2 lists the approximate thickness of the fresh/brackish water lens calculated from the elevation of the salt water interface interpreted from the individual TDEM soundings. The table includes the value of static water level (head) calculated by using the Ghyben-Herzberg principle.

Table 4-1. Hydrogeologic information derived from TDEM soundings (values in ft)

Sounding #	Surface Elevation	Elevation of Salt Water	Calculated Static Water Level (head)	Approximate Thickness of Fresh/ Brackish Water Lens
1	1400	-329	8	337
2	1505	-430	11	441
3	1645	-390	10	400
4	1560	-344	9	353
5	1405	-345	9	354
6	1560	-422	11	433
7	1660	-396	10	406
8	1720	Not Detected	N/A	N/A
9	1525	Not Detected	N/A	N/A
10	1400	Not Detected	N/A	N/A

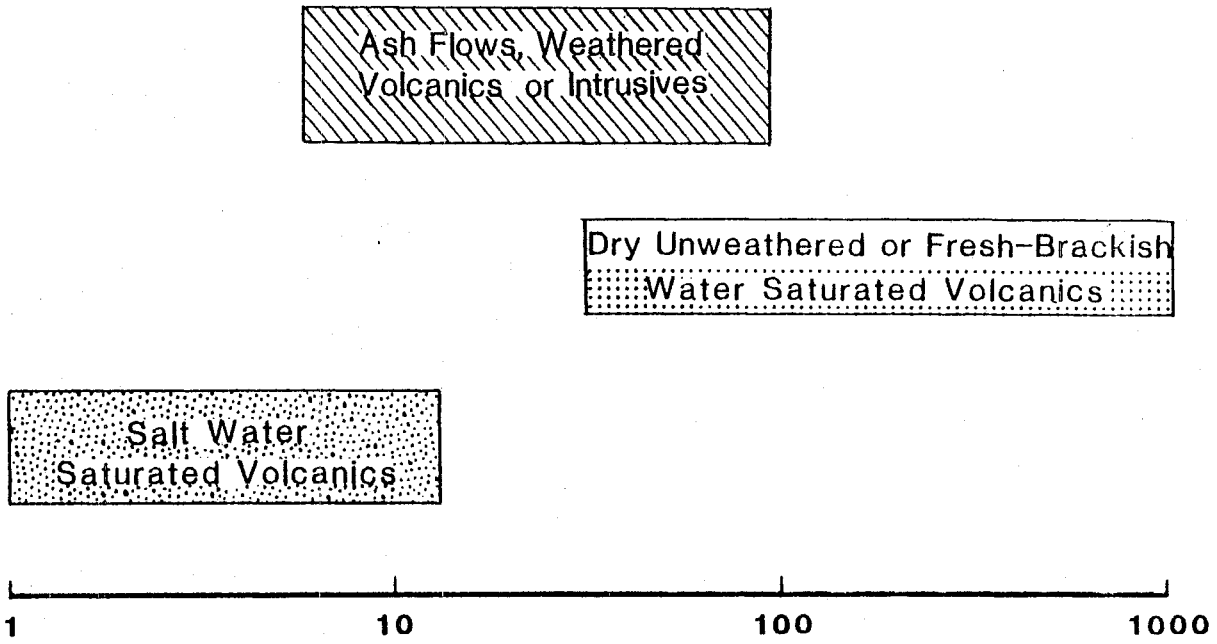

BLACKHAWK GEOSCIENCES, INC.

CHARACTERISTIC RESISTIVITY RANGES

DIVISION OF WATER RESOURCES MGMT.
STATE OF HAWAII

PROJECT NO: 91064 Figure 4-1

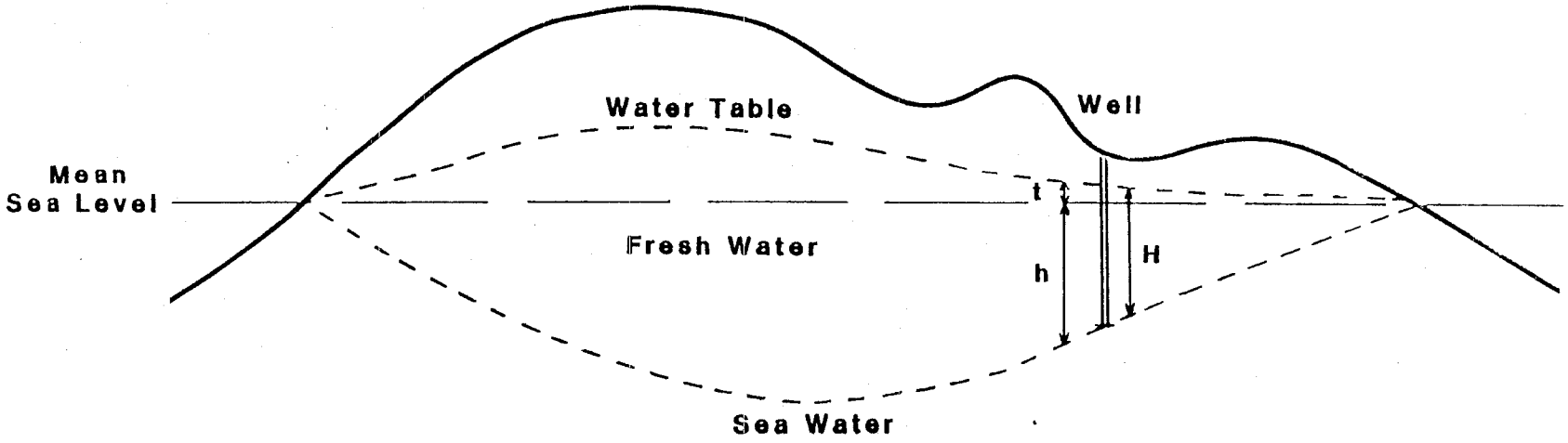

$t = 1/40\ (h)$

FROM: HERZBERG

BLACKHAWK GEOSCIENCES, INC.

Illustration of the
Ghyben-Herzberg Principle
DIVISION OF WATER RESOURCES MGMT.
STATE OF HAWAII

PROJECT NO: 91064 Figure 4-2

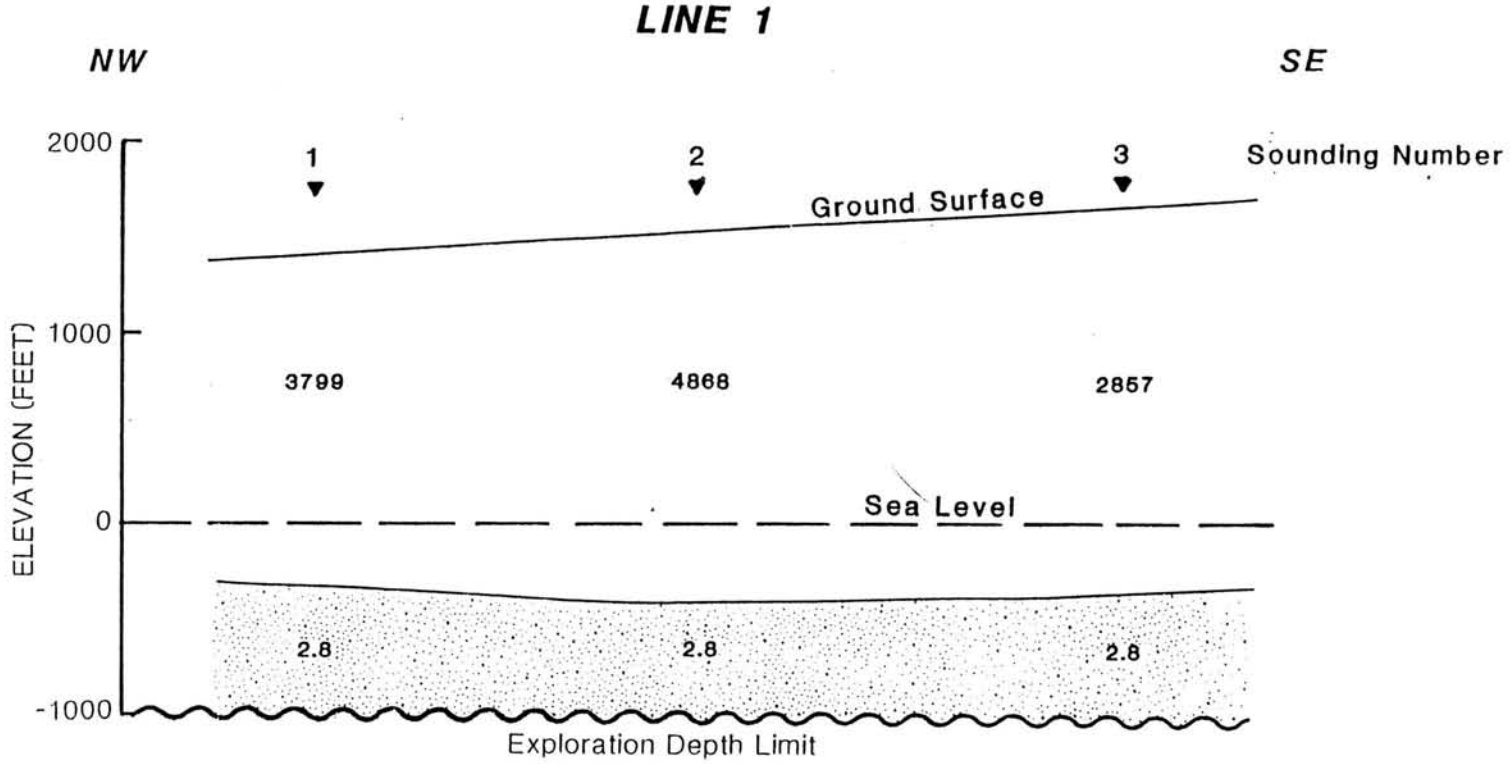
LINE 1
NW
SE
2000
1000
0
-1000
ELEVATION (FEET)
1
2
3
Sounding Number
Ground Surface
3799
4868
2857
Sea Level
2.8
2.8
2.8
Exploration Depth Limit

LINE 2

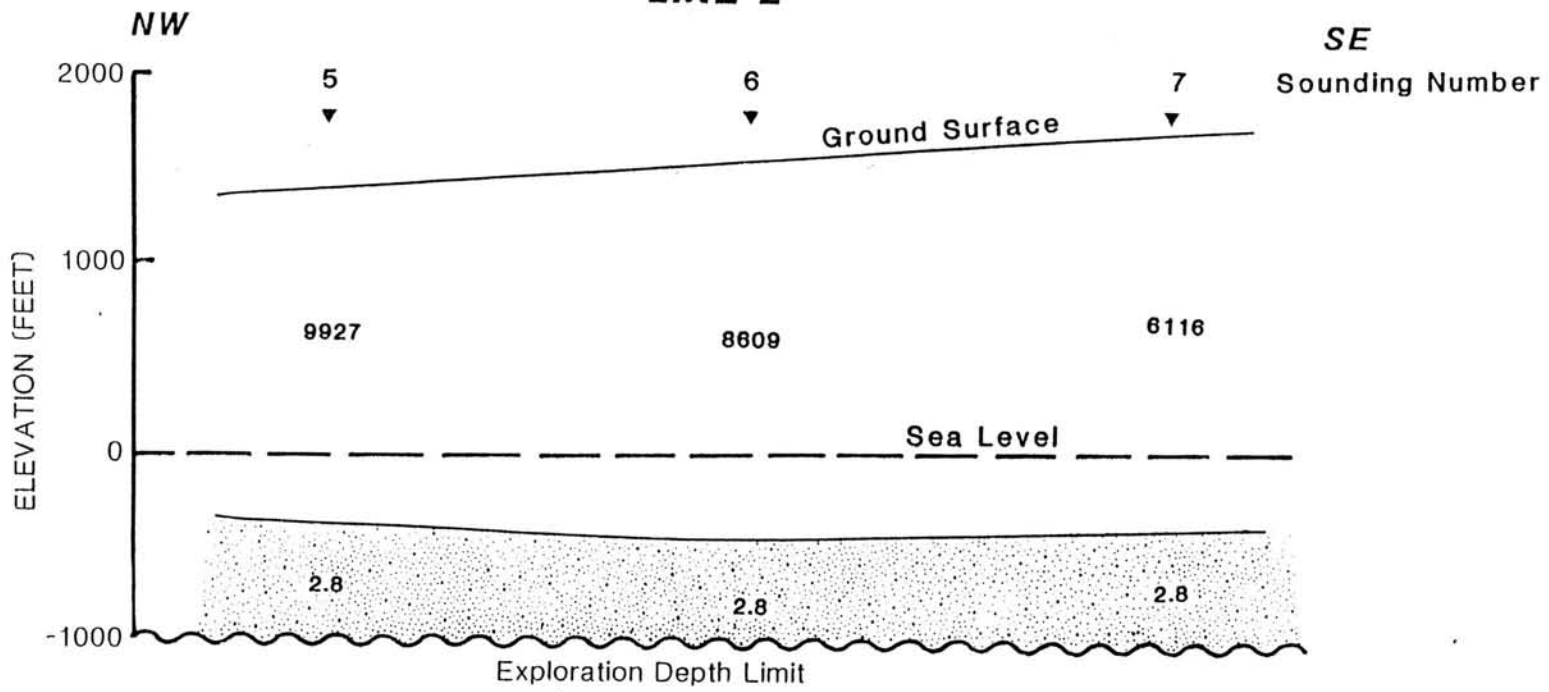

2.8 Resistivity, Ohm-m

Boundary of Resistivity Values

Inferred Geologic Structure

Unweathered or Fresh/Brackish Water Saturated Volcanics

Ash Flows, Weathered Volcanics or Change in Water Quality

Salt Water Saturated Volcanics

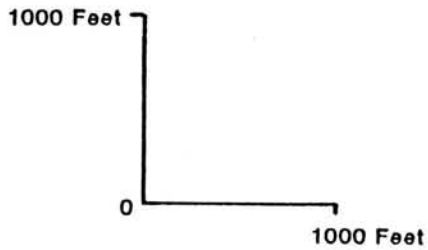

BLACKHAWK GEOSCIENCES, INC.

GEOELECTRIC CROSS SECTION
LINES 1 AND 2
DIVISION OF WATER RESOURCES MGMT.
STATE OF HAWAII

PROJECT NO: 91054 Figure 4-3

LINE 3

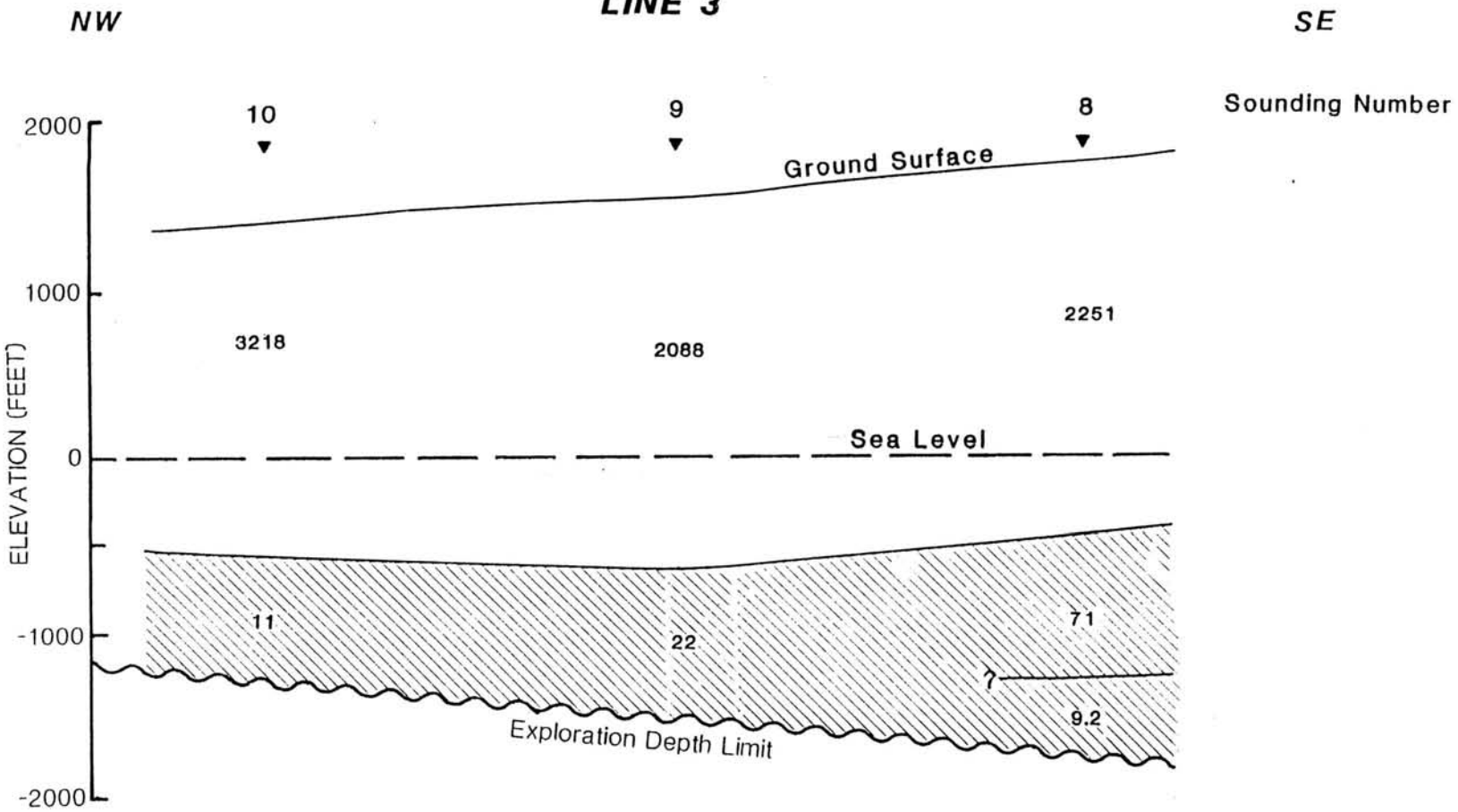

LINE 4

SW

NE

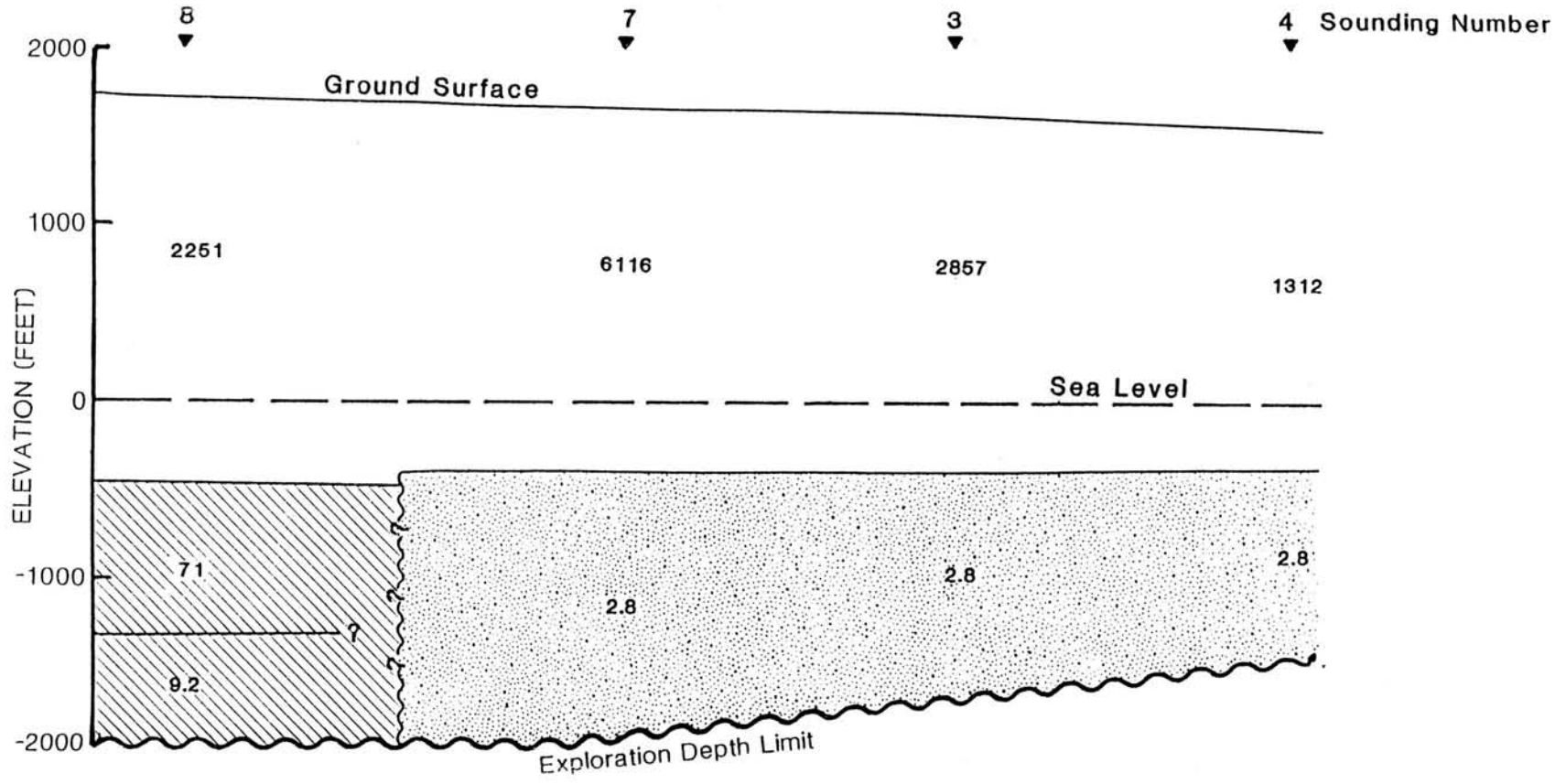

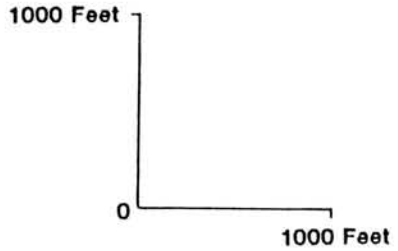

2.8 Resistivity, Ohm-m

Boundary of Resistivity Values

Inferred Geologic Structure

Unweathered or Fresh/Brackish Water Saturated Volcanics

Ash Flows, Weathered Volcanics or Change in Water Quality

Salt Water Saturated Volcanics

BLACKHAWK GEOSCIENCES, INC.

GEOELECTRIC CROSS SECTION
LINES 3 AND 4

DIVISION OF WATER RESOURCES MGMT.
STATE OF HAWAII

PROJECT NO: 91054

Figure 4-4

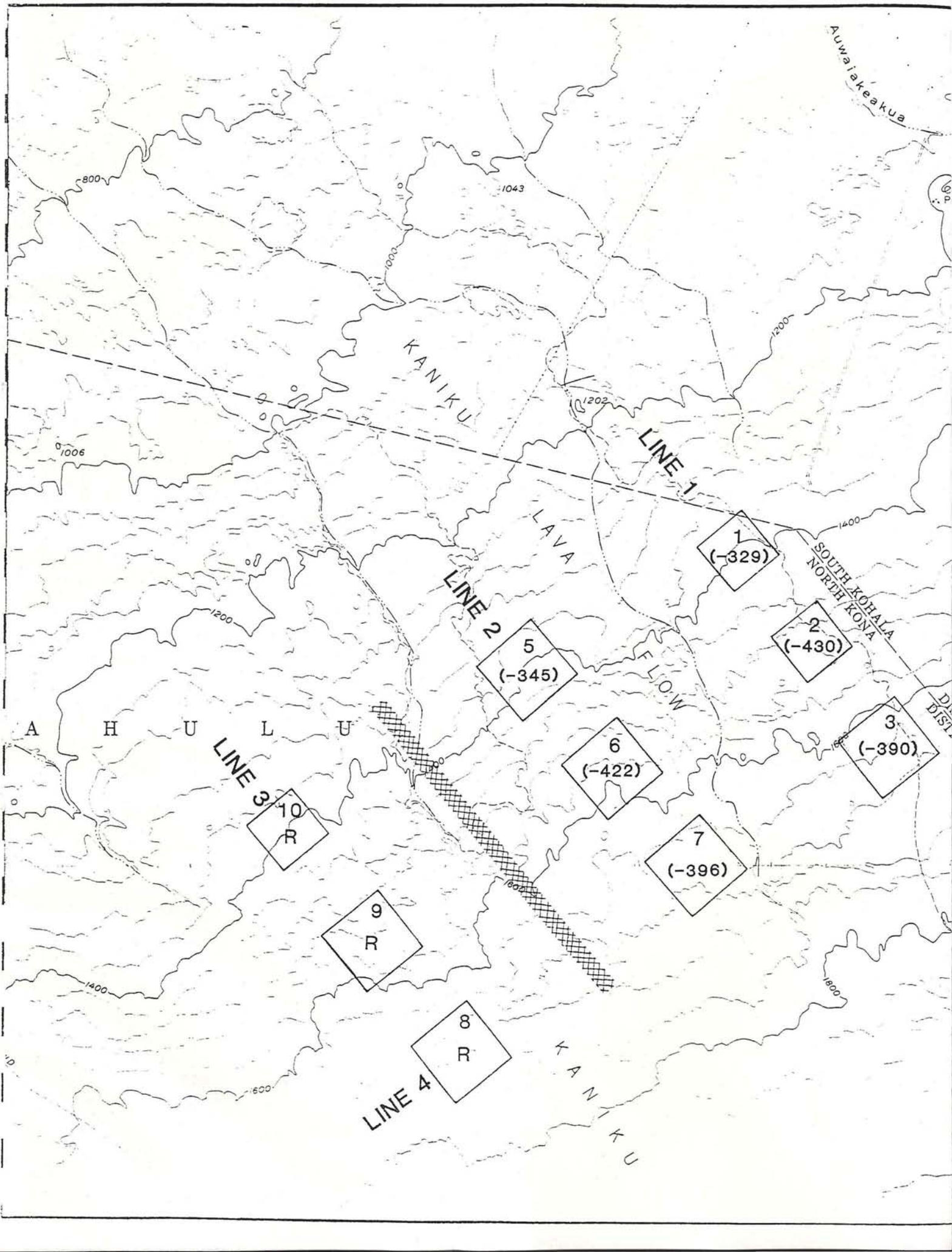
Auwaiakeakua
800
1043
1000
1200
KANIKU
1202
1006
LINE 1
1400
LAVA
LINE 2
1200
FLOW
A H U L U
LINE 3
1600
1400
1800
LINE 4
KANIKU
1600
1
(-329)
SOUTH KOHALA
NORTH KONA
2
(-430)
3
(-390)
5
(-345)
6
(-422)
7
(-396)
10
R
9
R
8
R

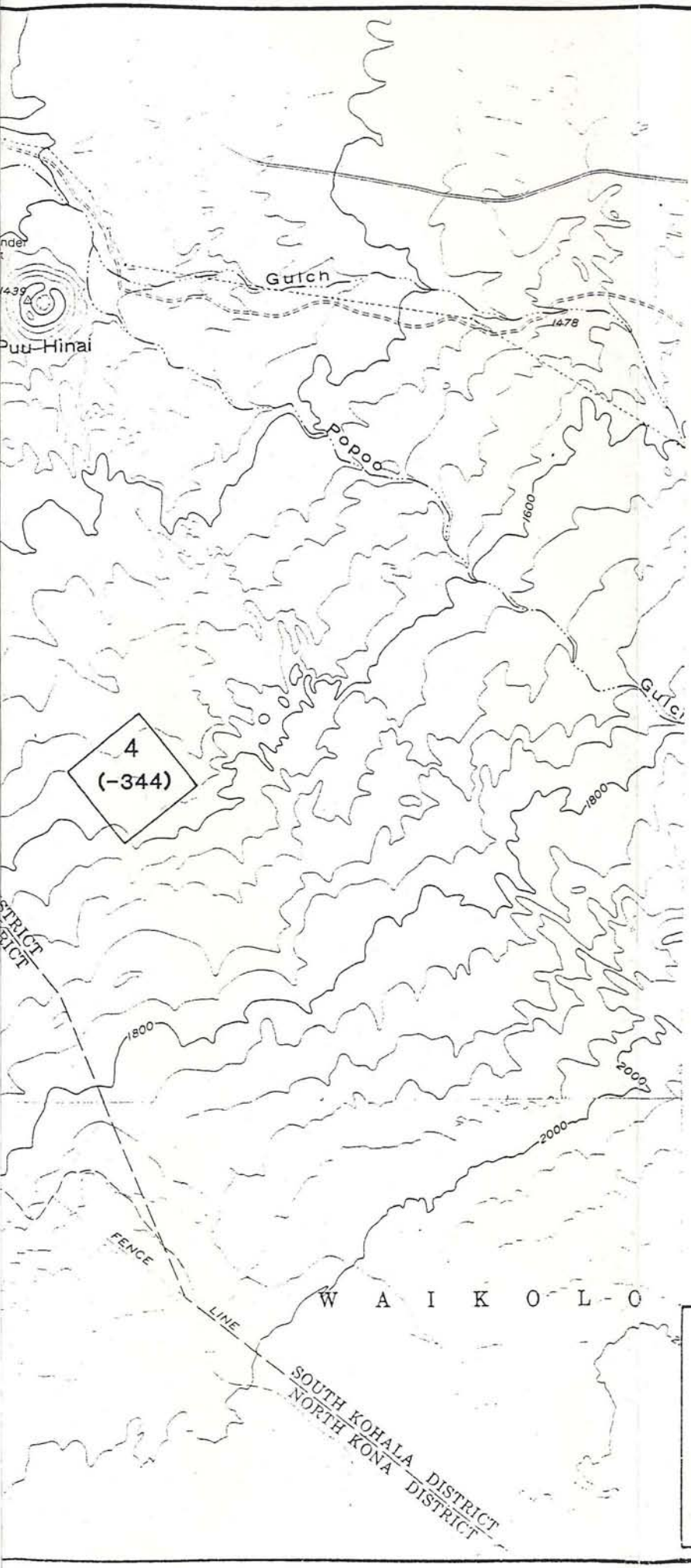

4 Sounding Location and Number

(-329) Approximate Elevation (in feet) of Top of Salt Water Inteface

R Resistive Basement

Approximate Location of Boundary Between Basal Mode Water and Areas Where a Resistive Basement was Detected

PUU HINAI AND PUU ANAHULU QUADRANGLES

0 2000 4000 Feet

BLACKHAWK GEOSCIENCES, INC.

TDEM INTERPRETATION MAP

DIVISION OF WATER RESOURCES MGMT.
STATE OF HAWAII

PROJECT NO: 91054 Figure 4-5

5.0 CONCLUSIONS AND RECOMMENDATIONS

The main objective of the TDEM survey was to assist in the ground water resource evaluation of the Puu Anahulu area of North Kona, Hawaii. The results of the TDEM survey are summarized in Figures 4-3, 4-4 and 4-5. As shown in Figure 4-5 (beneath soundings 1 through 7), salt water saturated volcanics were detected at depth and fresh/brackish ground water resources are expected to be present in the basal mode. The thickness of the basal fresh/brackish water lens is expected to vary from about 329 ft to 430 ft. Beneath soundings along Line 3 (10, 9 and 8) salt water saturated volcanics were not detected. The intermediate to high resistivity layer detected below sea level on these soundings may be caused by lithologic, geologic, or hydrologic variations and thus, estimates of available ground water resources cannot be made for these soundings. The depth and resistivities of the lower layer in these soundings display some similarities to soundings taken on previous surveys near a ground water damming structure. Thus, the potential for significant ground water resources may be present up-gradient of the structure if other favorable subsurface conditions exist, such as high porosity and permeability.

The location of the boundary between areas with basal mode ground water resources and areas where a resistive basement was detected is not accurately determined because of the large distances between lines and soundings in this vicinity of the study area. To better define the boundary location and its relative direction, additional soundings between Line 2 and Line 3 are recommended. To determine if high level ground water resources exist southwest of Line 3, additional soundings are recommended in this area.

The relative accuracy in determining the depth to the salt water saturated interface is expected to be about $\pm$ 5% of the total depth measured.

BLACKHAWK GEOSCIENCES, INC.
17301 WEST COLFAX AVE. SUITE 170 GOLDEN, CO 80401
PHONE (303) 278-8700 FAX (303) 278-0789

Transient Electromagnetic Soundings

GROUNDWATER
STRUCTURAL GEOLOGY
PERMAFROST
MINING
SHALLOW OIL AND GAS

INTRODUCTION

Electromagnetic transient methods for soundings have been used for many years in the U.S. and the U.S.S.R. for mapping structures for hydrocarbon and geothermal exploration. Transient sounding for shallow exploration (<1 km) was until recently not possible, due to the lack of an instrument with the necessary specifications. The situation has changed since the Geonics EM37 became commercially available. There are several important exploration objectives for shallow exploration using transient methods such as:

1) structural mapping for coal, oil sands and oil shales
2) structural mapping for mineral exploration
3) hydrogeological investigations
4) deep onshore and offshore permafrost mapping for design of well casings, facilities, and for static correction to seismic reflection data

These soundings are being made with separations between transmitter and receiver comparable to the depth of investigation, so that good lateral resolution is obtained.

These methods can be extended with similar equipment for such deeper exploration objectives (3 to 5 km) as:

a) mapping hydrocarbon-water contacts
b) mapping overthrust and thickness of volcanic covers
c) geothermal exploration

Examples of successfully using transient EM for some of these objectives are given in this note.

PHYSICAL PRINCIPLES

A transient system consists of a transmitter and a receiver. The transmitter configuration can be a non-grounded loop or a grounded line. The configuration used in most of our work has been the non-grounded loop. The sensors are multi-turn air coils with effective areas varying from 32 square meters to 1000 square meters. Figure 1 shows the transmitter-receiver arrangements used for transient soundings.

The current generated in the transmitter is shown in Figure 2. There are two periods of time, time-on and time-off. Measurements are made only during time-off. In accordance with Faraday's Law, an electromagnetic induction appears when the current in the transmitter varies with time. When the turn-off ramp is linear the induced electromotive force is a rectangular pulse.

The electromagnetic induction creates eddy currents in the ground. These induced currents are time-variant and cause a time-varying secondary magnetic field, which is measured as an electromotive force in the receiver coil. It has been shown that the induced currents are horizontal closed rings in the absence of lateral inhomogeneities (1). There is no vertical component of current flow. Figure 3 schematically illustrates the distribution of eddy currents as a function of depth at different times. This figure shows that current maxima move down with increasing time. The currents not only move down, but also out. The current expansion can be described by a diffusion type equation.

The electromotive force measured by the receiver coil is the result of the change of current flow with time. It is evident from Figure 3 that a measurement at time, to, will mainly be sensitive to the resistivity of near-surface layers. With increasing time, when the current maxima diffuse down, the electromotive force will progressively become more sensitive to the properties of deeper layers. Therefore, by making measurements as a function of time, information about the geoelectric section is obtained. In transient soundings effective exploration depth is dominantly a function of time rather than distance. This fact results in a high lateral resolution for transient soundings.

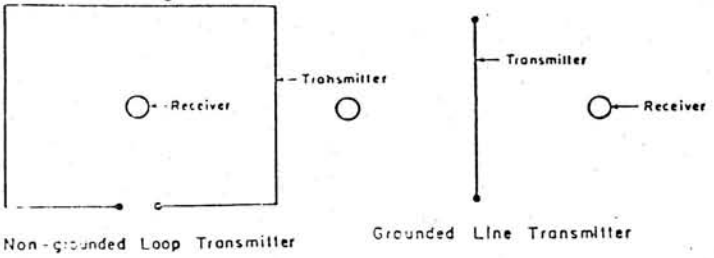

FIGURE 1. Different arrays of transmitter-receiver used in transient soundings.

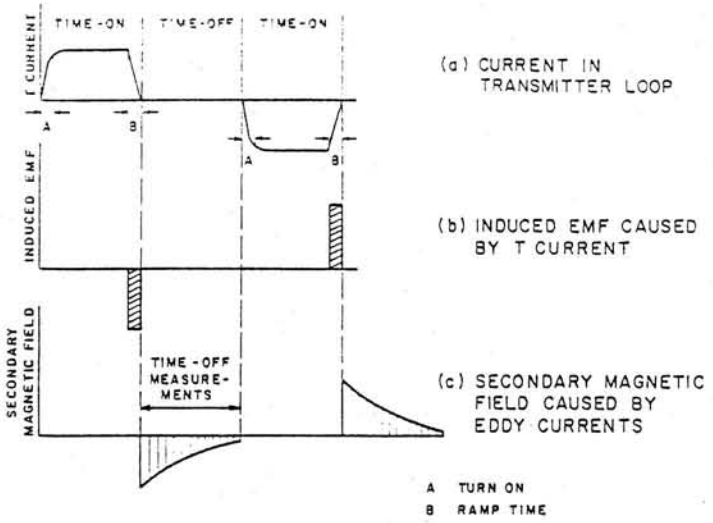

FIGURE 2. System Waveforms

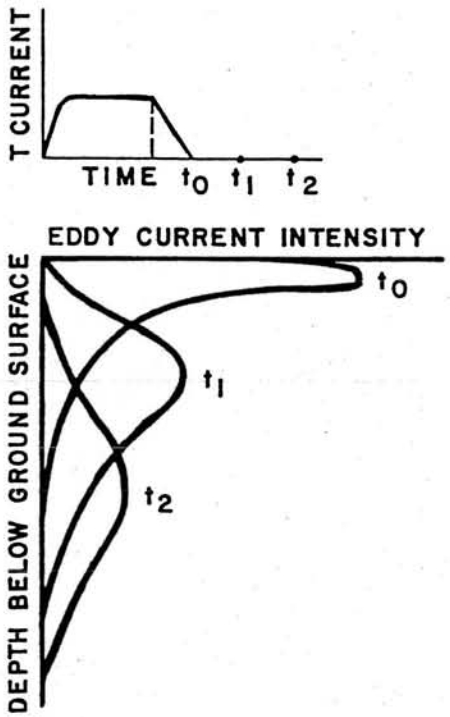

FIGURE 3. Schematic illustration of maximum current distribution intensity in a vertical plane.

Behavior of Field

Over certain ranges of time the transient field also has a higher sensitivity to the geoelectric section than other electrical methods. This fact can be understood from the behavior of the time derivative of the vertical component of the magnetic field over uniform half-space. In Figure 4, $\dot{B}_z$ is given as a function of the dimensionless parameter $\frac{\tau_1}{r}$.

where τ_1 $\tau_1 = \sqrt{2\pi\rho_1 t 10^7}$

and t is time after turn-off
ρ_1 is half-space resistivity

Several stages of time can be distinguished in the behavior of the electromotive force. At early time the emf is independent of time; there is an intermediate range of time in which the emf, rapidly decreases with time, and a late range of time in which the emf falls off as $t^{-5/2}$.

At early stage $\frac{\tau_1}{r} < 2$, and at late stage $\frac{\tau_1}{r} > 10$, the behavior of the field can be described by asymptotic expressions (1). The expressions are:

$$\text{early stage } \left(\frac{\tau_1}{r} < 2\right): \dot{B}^z = \frac{3m}{2\pi r^4} \cdot \rho_1 \qquad (1)$$

$$\text{late stage } \left(\frac{\tau_1}{r} > 10\right): \dot{B}^z = \frac{umr}{40\pi^{1/2} t^{5/2}} \cdot \frac{1}{\rho_1^{1/2}} \qquad (2)$$

It is evident that a measurement at late stage is more sensitive to ground resistivity than a measurement at early stage.

Late stage commences when $\frac{\tau_1}{r} > 10$. Thus, if r (transmitter-receiver separation) is kept small, late stage will commence in earlier time channels. The advantages of small transmitter-receiver separation, therefore, not only is a better lateral resolution, but also a higher sensitivity to the geoelectric section. This often results in a better vertical resolution.

Some of these advantages of transient soundings are lost when large transmitter-receiver separations are used. In the first place increasing separation will decrease lateral resolution. When larger separations are used the geoelectric section measured does not occur directly under the receiver, but will be influenced by the subsurface conditions between transmitter and receiver. Secondly, at large separations the behavior of the field will correspond to early stage, over a large time range, and the sensitivity to the geoelectric section will be less. This will decrease vertical resolution.

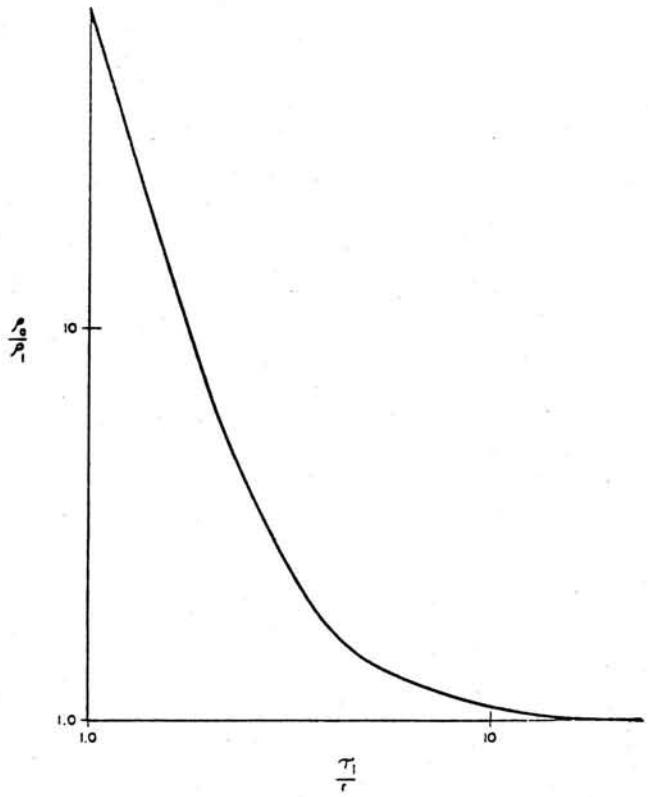

FIGURE 5. Late stage apparent resistivity curve of uniform ground.

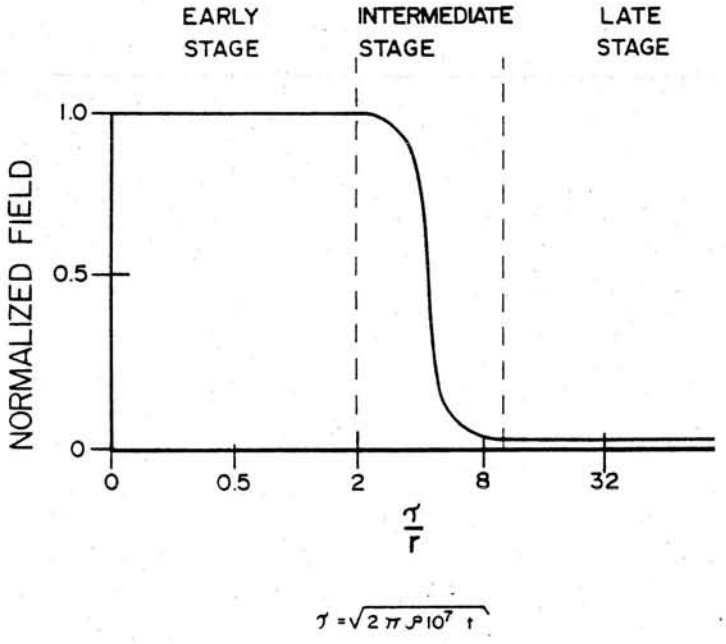

FIGURE 4. Behavior of time derivative of vertical magnetic field as a function of time.

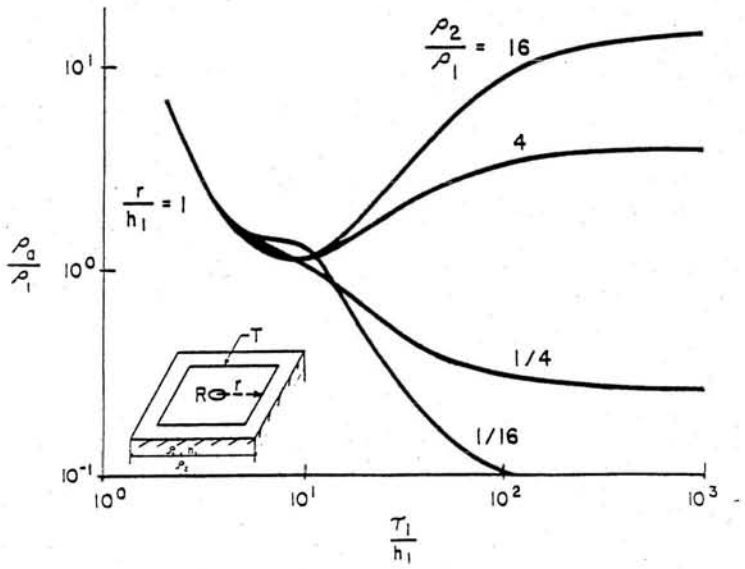

FIGURE 6. Late stage apparent resistivity curves for two-layered sections.

Definition of Apparent Resistivity

It is common in all electrical and electromagnetic methods to transform the fields measured into apparent resistivities. The purpose of that transformation is to obtain a convenient visualization of how the behavior of the field measured, differs from the behavior of the field over uniform half-space. Transient soundings are no exception. In direct current and magnetotelluric soundings the relation between measured signal, and resistivity of uniform half-space, is the same for all electrode spacings (direct current) and over the entire frequency range (magnetotelluric). In transient soundings the relation between resistivity of uniform half-space and measured signal is a function of time of measurement. It is evident from Figure 4 and equation 1 and 2 that there are two ranges of time over which that relation is constant, i.e. early stage and late stage. In these ranges of time the behavior of the field is described by the asymptotic expression in [1] and [2], and these expressions can be used to define the apparent resistivities, given below.

$$\text{Early Stage} \quad \rho = \frac{\dot{\beta}_z 2\pi r^4}{3m} \qquad (3)$$

$$\text{Late Stage} \quad \rho = \left(\frac{u\, r\, m}{40\pi^{3/2} t^{5/2}\, \dot{\beta}_z} \right)^{2/3} \qquad (4)$$

The definition used in practice depends on several factors. Generally, when the behavior of the field over the critical range of time corresponds to late stage behavior, the late stage [4] definition is used. This situation generally occurs when small transmitter-receiver separations are used. An early stage definition would be used, if the behavior of the field measured correspond to early stage behavior in the first layer.

Figures 5 and 6 show computed late stage apparent resistivity curves for uniform half-space, and for two-layered sections respectively. The apparent resistivity curves are plotted in terms of the dimensionless parameters,

$$\rho_a/\rho_1 \quad \text{and} \quad \frac{\tau_1}{h_1} \quad \left(\text{or} \quad \frac{\tau_1}{r}\right) .$$

In transient EM the parameter τ_1 plays a role similar to skin depth in frequency domain sounding, or electrode spacing in direct current sounding. For a certain section τ_1 is proportional to $t^{1/2}$.

First, consider the apparent resistivity curve for uniform half-space. With increasing time the apparent resistivity gradually approaches the true resistivity of the half-space. For example, when $\tau_{1/r} > 10$, ρ_a approaches ρ_1. At early time the apparent resistivity exceeds ρ_1 due to the fact that the field behavior has not reached "late stage", while the definition of apparent resistivity is based on "late stage". The early part of the curve, corresponds to the early stage behavior of the field and ρ_1 can be derived from this part of the curve also.

The interpretation of transient soundings is based on the analysis of apparent resistivity curves for 2-, and other multi-layered curves. Along with inversion methods using large sections of curves, many emperical techniques for deriving parameters of the geoelectric section from parts of the curves have been developed and tested by geophysicists in the U.S.S.R.

The behavior of two-layered curves are used for illustration in Figure 6. At early time $\frac{\tau_1}{r} < 2$ all curves merge into one, corresponding to the behavior of the field in the first layer. In this range of time the eddy currents are mainly concentrated in the first layer. From the behavior of the curve at early time information about ρ_1 can be obtained. With increasing time ρ_a/ρ_1 increases, when $\rho_2/\rho_1 > 1$, and decreases when $\rho_2/\rho_1 < 1$. In this range of time currents progressively penetrate the second layer. At later time the apparent resistivity approaches the basement resistivity. In this range of time most currents are concentrated in the basement.

The similarities between the behavior of apparent resistivity used in transient and other electrical soundings should now be evident. The root of time replaces L-spacing or frequency on the horizontal axis.

Case History - Mapping Hydrocarbon-Water Contacts (2)

The formation resistivities of petroleum bearing rocks is dominantly a function of porosity and the resistivities of the fluid (or gas) in the pores. Salt water is commonly found in all oil and gas fields, and the salinity of the water in the pores is invariably high. The formation resistivity of petroleum bearing rocks saturated with water is, therefore, generally low ($\sim$2 ohm-m). The resistivity rapidly increases when oil or gas replaces water in the producing formation.

These facts are illustrated in the four induction logs of a shallow gas producing field in Oklahoma in Figure 7. This figure shows that the resistivity in the producing horizon is less than 3 ohm-m when brine saturated, and more than 50 ohm-m when gas saturated. This significant change in resistivity was measured from the surface by transient EM soundings in shallow fields.

To measure the gas-water contact transmitter loops with dimensions of 1500 ft. by 1500 ft. were used and measurements were made in the center of the loops. Figure 8a and b shows apparent resistivity curves obtained over locations with hydrocarbon saturation and brine saturation in the producing horizons, respectively. The difference between these curves at later time is readily observed. The curve obtained over a location with salt water in the producing horizon shows a decrease in apparent resistivity at late time; the curve obtained over a location with gas saturation shows a slight increase in apparent resistivity at late time.

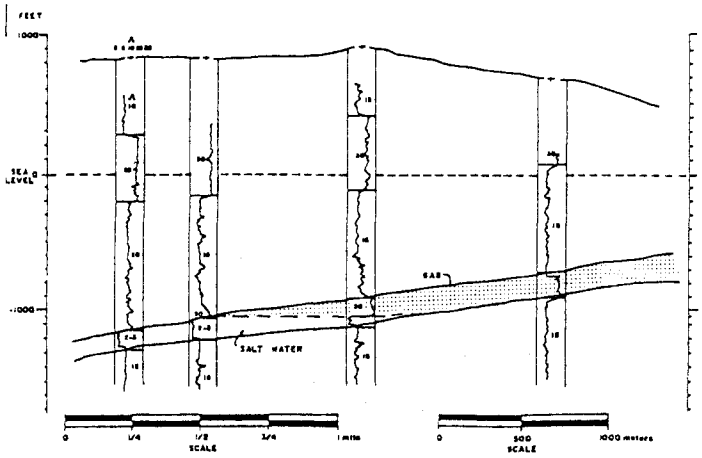

FIGURE 7. Geologic section with four induction logs of a shallow gas field in Oklahoma. The producing horizon occurs at depth of 1500 ft. to 2000 ft.

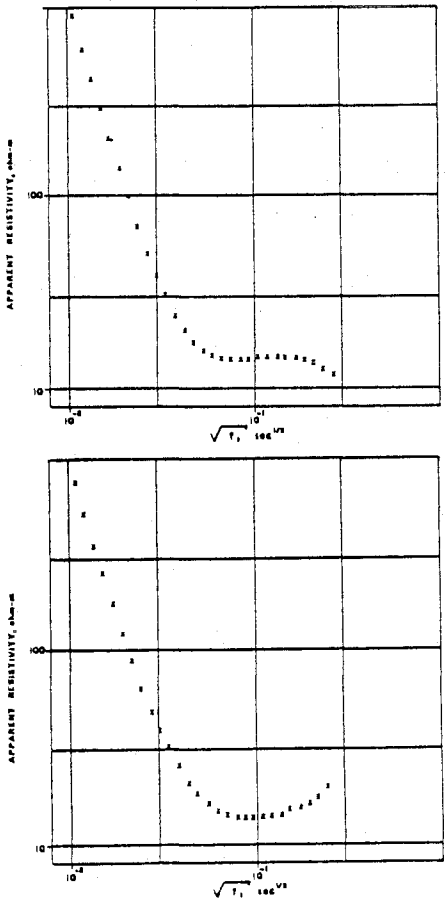

FIGURE 8. Transient apparent resistivity curves over a field in Oklahoma:
a) apparent resistivity curve over a location with salt water saturation
b) apparent resistivity curve over hydrocarbon saturation

From measurements at 11 transmitter loop positions a contour map of the conductance in the producing horizon could be made (Figure 9). Conductance is the product of the thickness of the formation and its conductivity (inverse of resistivity). The contour map derived from the measurements is consistent with the data of the four available induction logs.

Several similiar case histories are also found in the literature from the USSR. On the Siberian platform conductance contour maps of a horizon at depth of about 5000 ft. were constructed from transient soundings over a large area. Changes in conductance of producing horizons can have several causes. These are:

a) change in brine saturation of the pores (hydrocarbon accumulations)
b) change in lithology or porosity
c) disappearance or change in thickness of producing horizon

These conductance maps of producing horizons were used to compliment seismic interpretations to better define drilling targets.

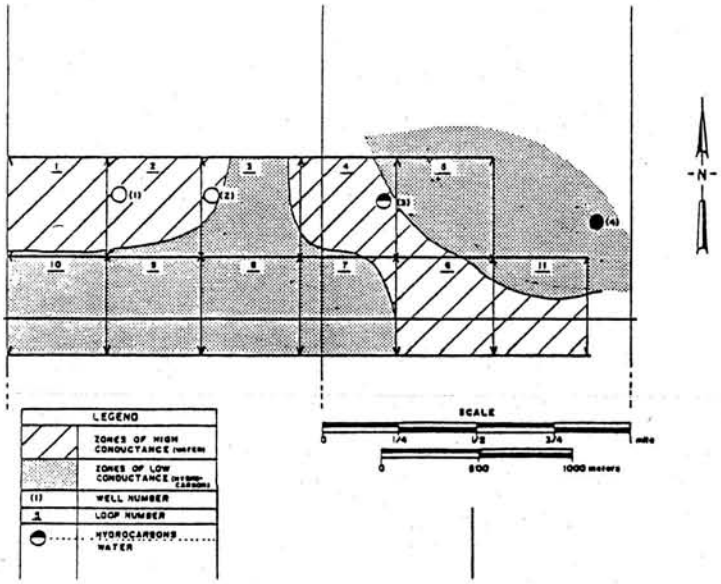

FIGURE 9. Contour conductance map of the producing formation derived from 11 transient soundings.

This case history can be used to illustrate the high sensitivity of transient sounding to the geoelectric section. In Figure 10 a, b, c computed apparent resistivity curves for the same section are shown for direct current, magnetotelluric and transient soundings. In both direct current and magnetotelluric soundings the presence of a conductive layer of 30 mhos would cause approximately 20 percent maximum change in apparent resistivity; for transient soundings the maximum change would be 45 percent. Moreover, it is clear from equation 2 that a 45 percent change in resistivity, will cause a 60 percent change in measured electromotive force. The sensitivity of transient EM to the presence of a conductive layer is approximately three times that of other electrical methods.

It was discussed that lateral resolution in transient soundings to a large extent is a function of transmitter-receiver separation. In the survey in Oklahoma measurements were also made with the receiver outside the transmitter loop, 500m from the center. From curves outside the loop the brine-hydrocarbon contact could not be determined. **It clearly illustrated that the effective geoelectric section is not measured under the receiver, but is affected by the subsurface conditions between transmitter and receiver. Increasing transmitter-receiver separation decreases lateral resolution.**

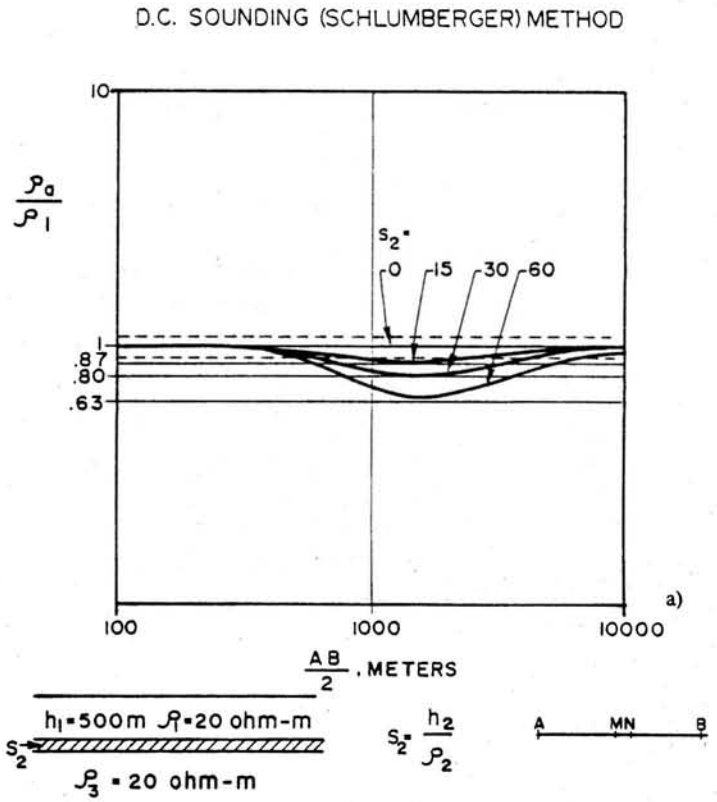

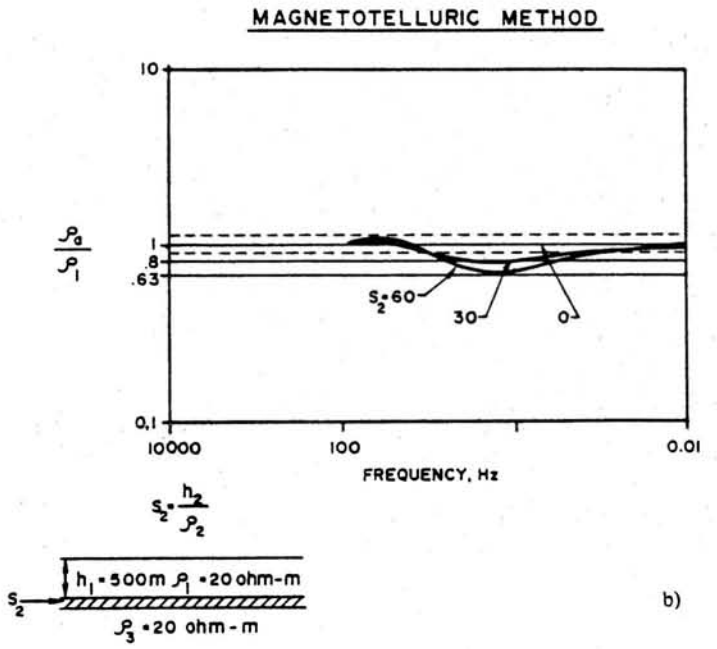

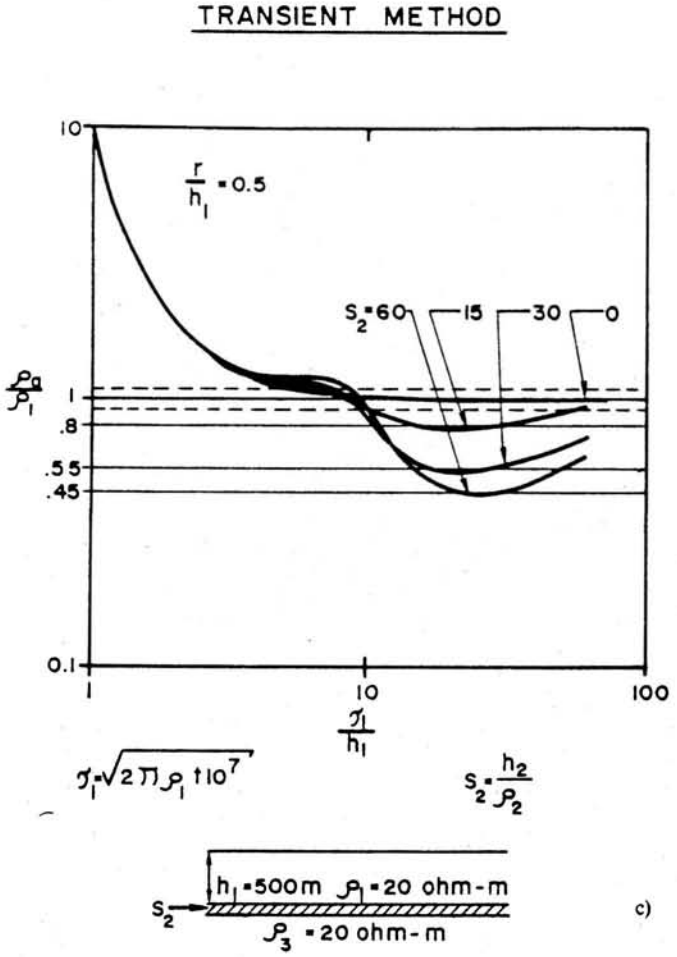

FIGURE 10. Computed apparent resistivity curves for geoelectric section shown:
a) direct current
b) magnetotelluric
c) transient

Case History Onshore and Offshore Permafrost Mapping (3)

The thickness of permafrost along the coast of the Beaufort Sea may reach 2000 ft. The permafrost distribution is variable, particularly near water bodies. Offshore permafrost has been found to exist tens of kilometers from the shore line. The permafrost distribution is required for static correction to seismic reflection data, and for design of well casings and facilities. The increase in resistivity upon freezing is the basis for electrical methods to map permafrost.

Blackhawk Geo has performed hundreds of transient soundings in Alaska and Canada for onshore and offshore permafrost mappings. Figure 11 shows a section of permafrost traversing the coast line passing by the Gull Island well near Prudhoe Bay (4). Above the section the measured apparent resistivity curves are shown.

The section shows that on land permafrost is approximately 2000 ft. thick and has an average resistivity of about 400 ohm-m. The unfrozen ground underneath the permafrost has a resistivity of 2.5 ohm-m. Offshore the top to the permafrost falls off rapidly to 250m about 3 km from the shore line. The unfrozen sediments above the permafrost are saturated with brine and have a resistivity less than 2 ohm-m.

The case history illustrates the ability of transient EM to detect a resistive layer under thick conductive sections. High resolution marine seismic methods sometimes can map top to permafrost, with transient EM both top and bottom could be determined.

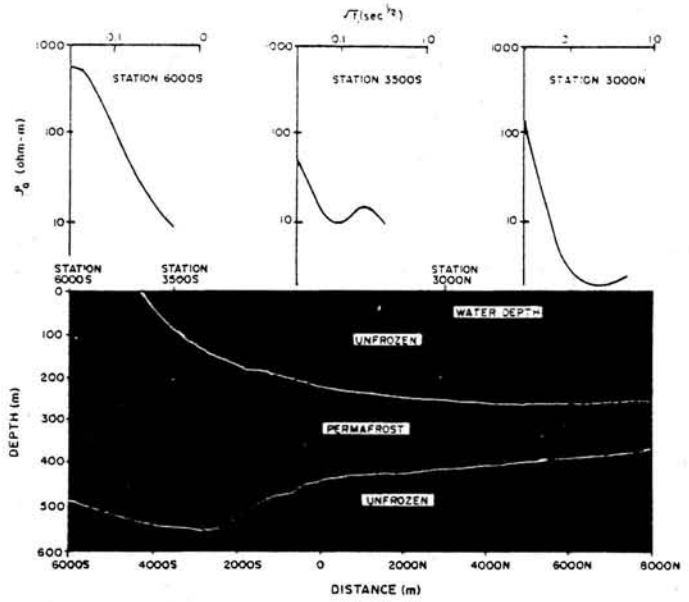

FIGURE 11. Permafrost section with apparent resistivity curves.

Case History - Mapping Depth to Basement

In northern British Columbia a survey was performed in support of a coal exploration program. The objective of transient sounding was to determine the thickness of the sedimentary rock overlaying the crystalline basement, and the contact of sedimentary and volcanic rock.

The geoelectric and geologic section derived from the various soundings is given in Figure 12. In addition to the geologic cross-section the longitudinal resistivity, $\rho\ell$, above the basement is shown. It was computed from the relation:

$$\rho\ell = \frac{H}{\frac{H1}{\rho_1} + \frac{H2}{\rho_2}}$$

where H is total thickness of sedimentary section
and H1, H2 are thicknesses of layer 1 and 2, respectively

The behavior of $\rho\ell$ shows a relatively constant value of about 20 ohm-m from Station 2200m to Station 1200m. From Station 1200m to 200m, $\rho\ell$ increases to a maximum value of about 60 ohm-m. The increase in $\rho\ell$ at Station 1200m was interpreted as the contact of sedimentary and volcanic rock. This interpretation was consistent with the information obtained from two drillholes placed on the cross-section. The drillholes did not penetrate into basement rock.

The section of Figure 12 was largely derived from soundings in the center of 100m by 100m loops.

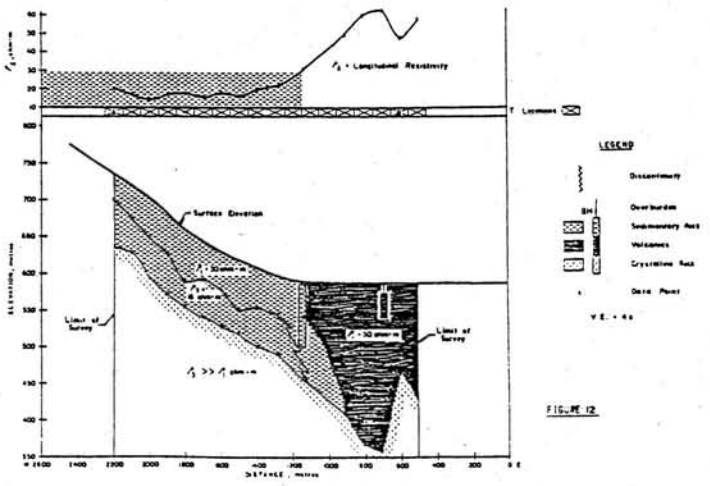

FIGURE 12. Geoelectric section derived from transient soundings.

References

1) Kaufman, A.A., and Keller, G.V., **Frequency and Transient Soundings, Elsevier,** (1983).

2) Wightman, W.E., Kaufman, A.A., and Hoekstra, P., Mapping Gas-Water Contacts in Shallow Producing Formations with Transient EM, paper presented to 53rd Annual Meeting SEG, Las Vegas, (1983).

3) Ehrenbard, R.L., Hoekstra, P., and Rozenberg, G., Transient EM for Permafrost Mapping, Proc. 4th Int. Conf. Permafrost, Fairbanks, Ak, (1983).

4) Osterkamp, T.E. and Payne, M.W., Estimates of Permafrost Thickness from Well Logs in Northern Alaska, Cold Regions Sci. and Techn. V. 5 (1981), pp. 13-17.

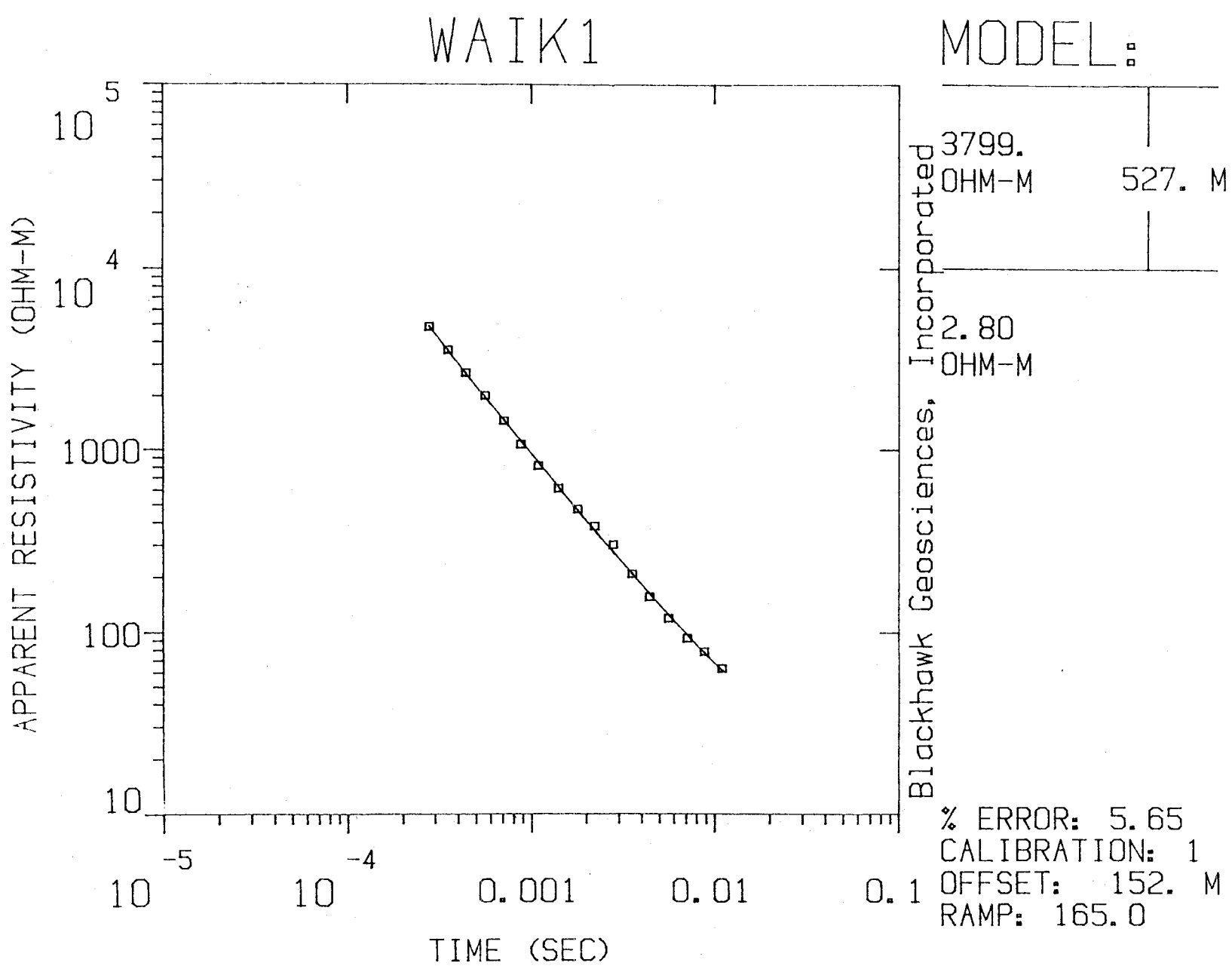
WAIK1
MODEL:
3799.
OHM-M
527. M
2.80
OHM-M
APPARENT RESISTIVITY (OHM-M)
10^5
10^4
1000
100
10
10^-5
10^-4
0.001
0.01
0.1
TIME (SEC)
Blackhawk Geosciences, Incorporated
% ERROR: 5.65
CALIBRATION: 1
OFFSET: 152. M
RAMP: 165.0

MODEL: 2 LAYERS

RESISTIVITY (OHM-M)	THICKNESS (M)	ELEVATION (M)	ELEVATION (FEET)	CONDUCTANCE (S) LAYER	CONDUCTANCE (S) TOTAL
		426.7	1400.0		
3799.13	527.1	-100.3	-329.2	0.1	0.1
2.80					

	TIMES	DATA	CALC	% ERROR	STD ERR
1	2.80E-04	4.83E+03	4.86E+03	-0.654	
2	3.55E-04	3.60E+03	3.56E+03	1.000	
3	4.43E-04	2.69E+03	2.67E+03	0.857	
4	5.64E-04	2.00E+03	1.96E+03	2.250	
5	7.13E-04	1.44E+03	1.45E+03	-0.730	
6	8.81E-04	1.06E+03	1.11E+03	-4.274	
7	1.10E-03	8.14E+02	8.49E+02	-4.062	
8	1.41E-03	6.13E+02	6.22E+02	-1.346	
9	1.80E-03	4.72E+02	4.64E+02	1.701	
10	2.22E-03	3.81E+02	3.60E+02	5.959	
11	2.80E-03	3.01E+02	2.74E+02	9.748	
12	3.55E-03	2.08E+02	2.09E+02	-0.474	
13	4.43E-03	1.56E+02	1.62E+02	-3.839	
14	5.64E-03	1.19E+02	1.24E+02	-3.962	
15	7.13E-03	9.24E+01	9.65E+01	-4.237	
16	8.81E-03	7.81E+01	7.70E+01	1.406	
17	1.10E-02	6.32E+01	6.15E+01	2.708	

R: 152. X: 0. Y: 152. DL: 305. REQ: 169. CF: 1.0000
TDHZ ARRAY, 17 DATA POINTS, RAMP: 165.0 MICROSEC, DATA: NAIK1
2910 1111 1111 2 OPR XTL L 6 10+1000
Ch.21 = 0.165 Ch.22 = 0.89 Ch.23 = 15 Ch.24 = 9
RMS LOG ERROR: 2.39E-02, ANTILOG YIELDS 5.6524 %
LATE TIME PARAMETERS

* Blackhawk Geosciences, Incorporated *

PARAMETER RESOLUTION MATRIX:
"F" MEANS FIXED PARAMETER
P 1 0.97
P 2 0.00 0.00
F 1 0.00 0.00 1.00
P 1 P 2 F 1

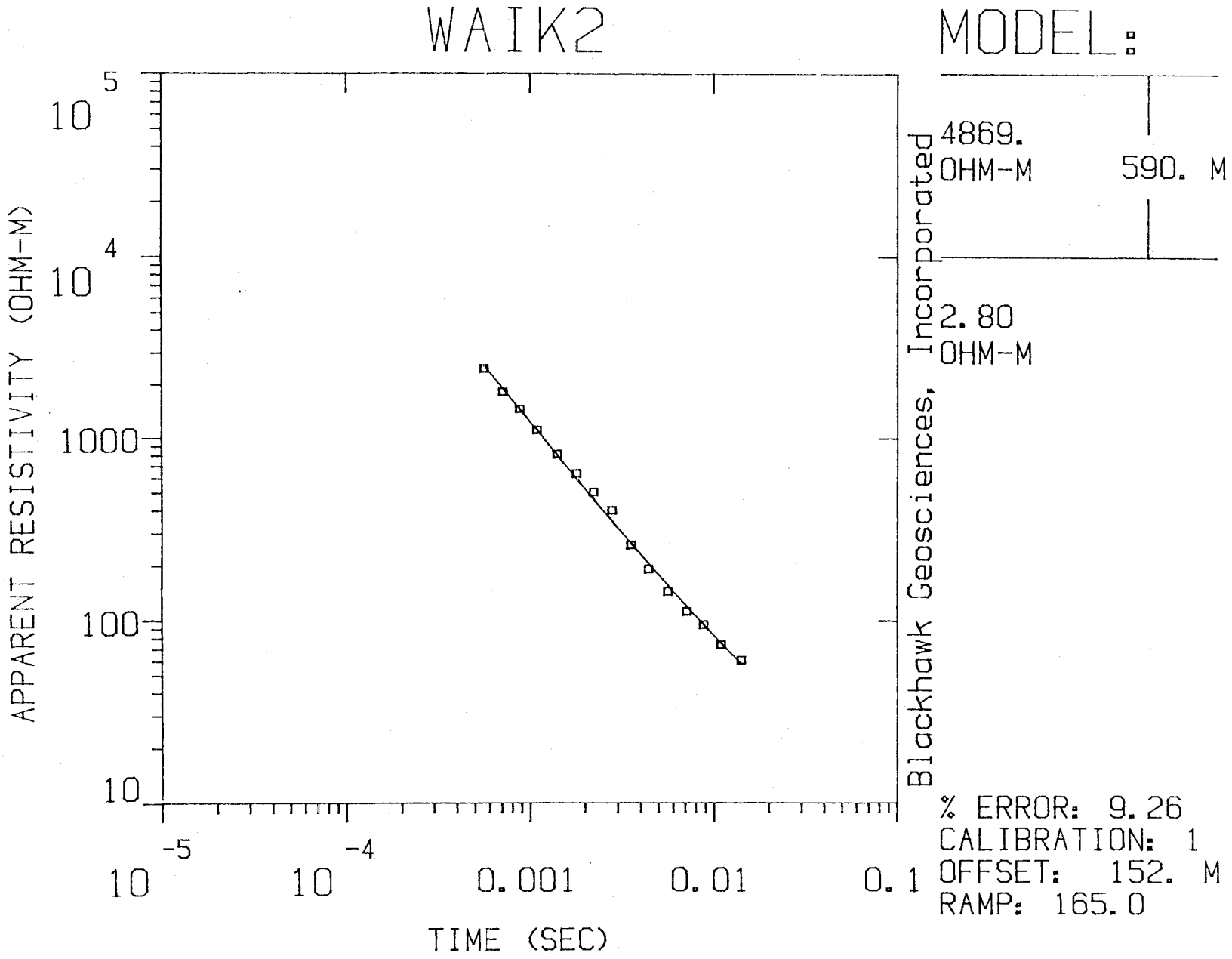
WAIK2
MODEL:
APPARENT RESISTIVITY (OHM-M)
10^5
10^4
1000
100
10
10^-5
10^-4
0.001
0.01
0.1
TIME (SEC)
4869.
OHM-M
590. M
2.80
OHM-M
Blackhawk Geosciences, Incorporated
% ERROR: 9.26
CALIBRATION: 1
OFFSET: 152. M
RAMP: 165.0

MODEL: 2 LAYERS

RESISTIVITY (OHM-M)	THICKNESS (M)	ELEVATION (M)	ELEVATION (FEET)	CONDUCTANCE (S) LAYER	CONDUCTANCE (S) TOTAL
		458.7	1505.0		
4860.63	589.8	-131.1	-430.2	0.1	0.1
2.80					

	TIMES	DATA	CALC	% ERROR	STD ERR
1	5.64E-04	2.46E+03	2.58E+03	-4.373	
2	7.13E-04	1.82E+03	1.90E+03	-4.246	
3	8.81E-04	1.46E+03	1.46E+03	-0.163	
4	1.10E-03	1.11E+03	1.11E+03	0.603	
5	1.41E-03	8.10E+02	8.00E+02	1.157	
6	1.80E-03	6.39E+02	6.02E+02	6.170	
7	2.22E-03	5.07E+02	4.63E+02	9.435	
8	2.80E-03	4.02E+02	3.52E+02	14.250	
9	3.55E-03	2.59E+02	2.66E+02	-2.594	
10	4.43E-03	1.92E+02	2.06E+02	-6.940	
11	5.64E-03	1.45E+02	1.36E+02	-7.452	
12	7.13E-03	1.13E+02	1.20E+02	-6.319	
13	8.81E-03	9.49E+01	9.53E+01	-0.459	
14	1.10E-02	7.40E+01	7.55E+01	-1.915	
15	1.41E-02	6.07E+01	5.79E+01	4.901	

R: 152. X: 0. Y: 152. DL: 305. REQ: 169. CF: 1.0000
TDHZ ARRAY, 15 DATA POINTS, RAMP: 160.0 MICROSEC, DATA: WAIK2
2910 1111 2222 2 OPR XTL L 6 10+1000
Ch.21 = 0.165 Ch.22 = 0.89 Ch.23 = 15 Ch.24 = 9
RMS LOG ERROR: 3.85E-02, ANTILOG YIELDS 9.2633 %
LATE TIME PARAMETERS

* Blackhawk Geosciences, Incorporated *

PARAMETER RESOLUTION MATRIX:
"F" MEANS FIXED PARAMETER
P 1 0.04
F 2 0.00 0.00
T 1 0.00 0.00 1.00
P 1 F 2 T 1

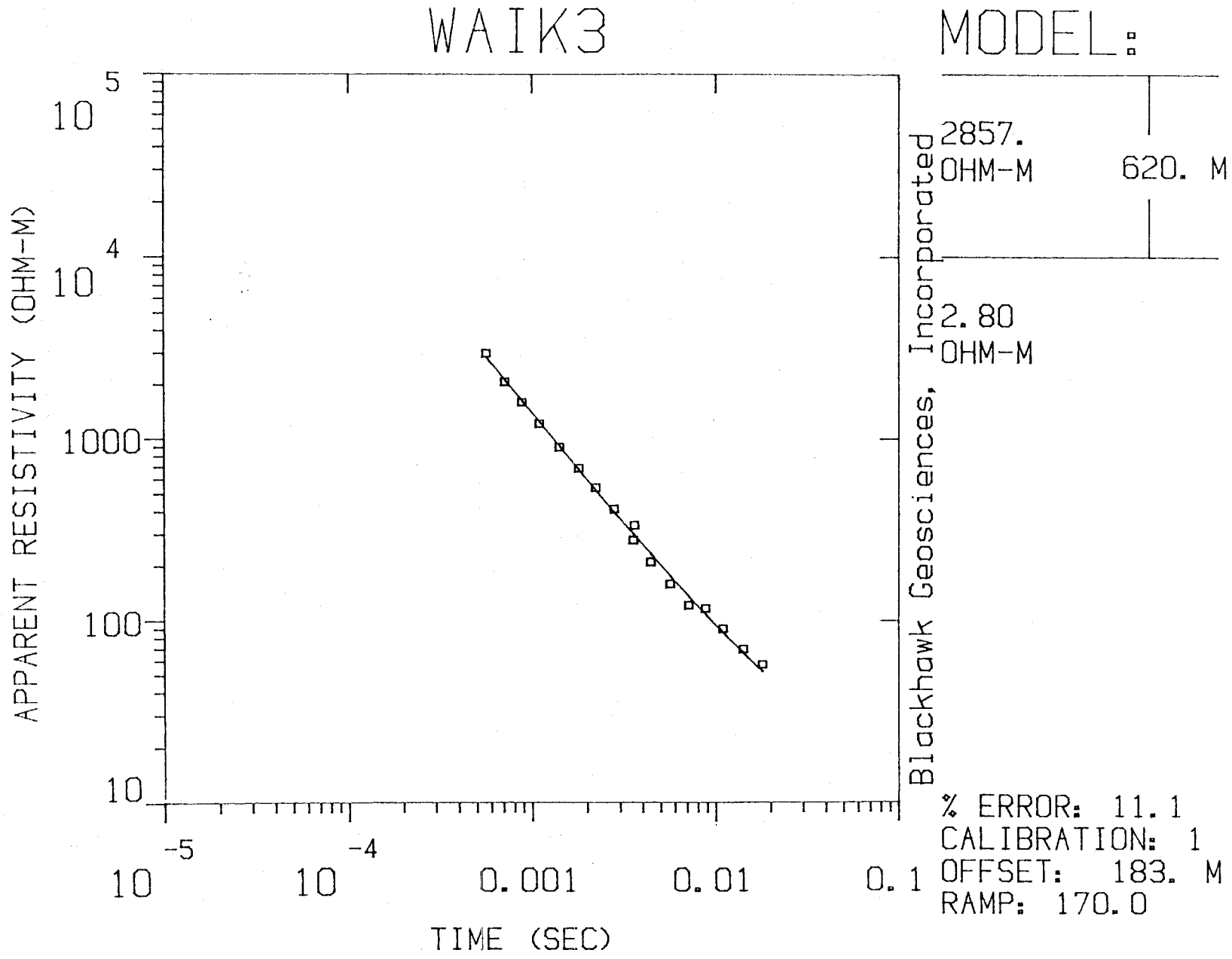
WAIK3
MODEL:
APPARENT RESISTIVITY (OHM-M)
10^5
10^4
1000
100
10
10^-5
10^-4
0.001
0.01
0.1
TIME (SEC)
2857.
OHM-M
620. M
2.80
OHM-M
Blackhawk Geosciences, Incorporated
% ERROR: 11.1
CALIBRATION: 1
OFFSET: 183. M
RAMP: 170.0

MODEL: 2 LAYERS

RESISTIVITY (OHM-M)	THICKNESS (M)	ELEVATION (M)	(FEET)	CONDUCTANCE (S) LAYER	TOTAL
		001.4	1643.0		
2857.34	620.1	-118.7	-389.4	0.2	0.2
2.80					

	TIMES	DATA	CALC	% ERROR	STD ERR
1	5.64E-04	2.98E+03	2.86E+03	4.063	
2	7.13E-04	2.06E+03	2.13E+03	-3.195	
3	8.81E-04	1.59E+03	1.63E+03	-2.487	
4	1.10E-03	1.20E+03	1.24E+03	-2.986	
5	1.41E-03	8.96E+02	9.10E+02	-1.572	
6	1.80E-03	6.87E+02	6.76E+02	1.615	
7	2.22E-03	5.40E+02	5.23E+02	3.206	
8	2.80E-03	4.13E+02	3.97E+02	3.961	
9	3.59E-03	2.76E+02	3.00E+02	-8.063	
10	3.60E-03	3.36E+02	2.96E+02	13.669	
11	4.43E-03	2.10E+02	2.33E+02	-9.979	
12	5.64E-03	1.59E+02	1.77E+02	-11.052	
13	7.13E-03	1.22E+02	1.36E+02	-10.851	
14	8.81E-03	1.17E+02	1.08E+02	7.517	
15	1.10E-02	9.02E+01	8.60E+01	4.876	
16	1.41E-02	6.95E+01	6.65E+01	4.584	
17	1.80E-02	5.71E+01	5.22E+01	9.383	

R: 183. X: 0. Y: 183. DL: 366. REQ: 203. CF: 1.0000
TDHZ ARRAY, 17 DATA POINTS, RAMP: 1720.0 MICROSEC, DATA: MAIK3
3010 1111 0003 Z OPR XTL L 7 10+1000
Ch.21 = 0.17 Ch.22 = 0.89 Ch.23 = 13 Ch.24 = 13
RMS LOG ERROR: 4.57E-02, ANTILOG YIELDS 11.1009 %
LATE TIME PARAMETERS

PARAMETER RESOLUTION MATRIX:
"F" MEANS FIXED PARAMETER
F 1 0.75
F 2 0.00 0.00
T 1 0.00 0.00 1.00
F 1 F 2 T 1

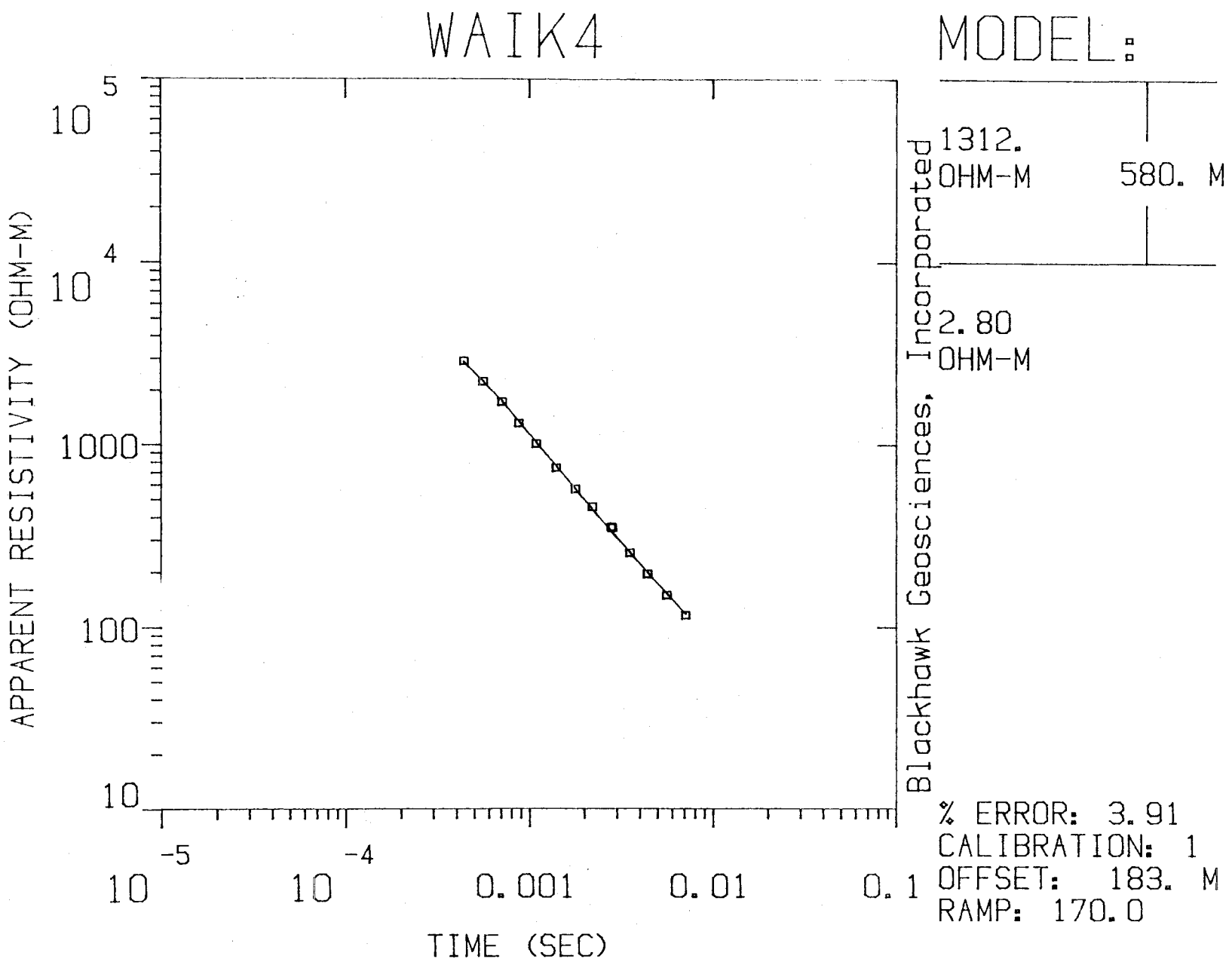
WAIK4
MODEL:
1312.
OHM-M
580. M
2.80
OHM-M
Blackhawk Geosciences, Incorporated
% ERROR: 3.91
CALIBRATION: 1
OFFSET: 183. M
RAMP: 170.0
APPARENT RESISTIVITY (OHM-M)
10^5
10^4
1000
100
10
10^-5
10^-4
0.001
0.01
0.1
TIME (SEC)

MODEL: 2 LAYERS

RESISTIVITY (OHM-M)	THICKNESS (M)	ELEVATION (M)	ELEVATION (FEET)	CONDUCTANCE (S) LAYER	CONDUCTANCE (S) TOTAL
		470.5	1560.0		
1512.34	580.3	-104.8	-343.8	0.4	0.4
2.50					

	TIMES	DATA	CALC	% ERROR	STD ERR
1	4.43E-04	2.91E+03	2.88E+03	0.879	
2	5.64E-04	2.34E+03	2.35E+03	-0.463	
3	7.13E-04	1.72E+03	1.75E+03	-1.338	
4	8.81E-04	1.31E+03	1.34E+03	-2.021	
5	1.10E-03	1.01E+03	1.03E+03	-1.556	
6	1.41E-03	7.46E+02	7.61E+02	-1.954	
7	1.80E-03	5.71E+02	5.71E+02	0.002	
8	2.22E-03	4.57E+02	4.42E+02	3.356	
9	2.80E-03	3.56E+02	3.38E+02	5.114	
10	2.85E-03	3.50E+02	3.32E+02	5.489	
11	3.55E-03	2.55E+02	2.57E+02	-0.905	
12	4.43E-03	1.95E+02	2.00E+02	-2.287	
13	5.64E-03	1.50E+02	1.53E+02	-2.154	
14	7.13E-03	1.16E+02	1.19E+02	-1.748	

R: 183. X: 0. Y: 183. DL: 366. REQ: 203. CF: 1.0000
TDHZ ARRAY, 14 DATA POINTS, RAMP: 170.0 MICROSEC, DATA: WAIK4
3010 0000 0003 2 OPR XTL L 7 10+1000
Ch.21 = 0.17 Ch.22 = 0.69 Ch.23 = 13 Ch.24 = 13
RMS LOG ERROR: 1.67E-02, ANTILOG YIELDS 3.9150 %
LATE TIME PARAMETERS

* Blackhawk Geosciences, Incorporated *

PARAMETER RESOLUTION MATRIX:
"F" MEANS FIXED PARAMETER

	P 1	F 2	T 1
P 1	1.00		
F 2	0.00	0.00	
T 1	0.00	0.00	1.00

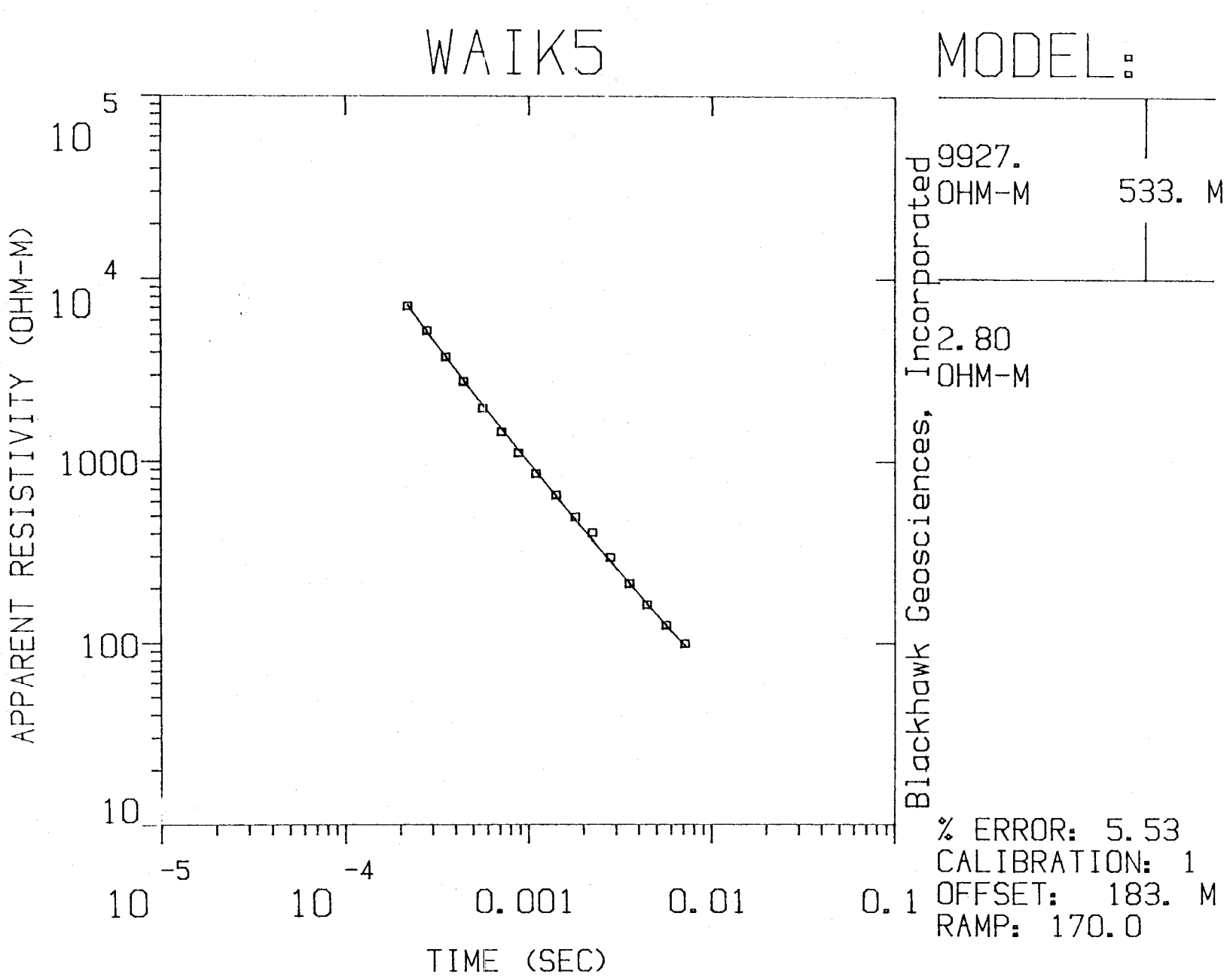
WAIK5
MODEL:
APPARENT RESISTIVITY (OHM-M)
10^5
10^4
1000
100
10
10^-5
10^-4
0.001
0.01
0.1
TIME (SEC)
9927.
OHM-M
533. M
2.80
OHM-M
Blackhawk Geosciences, Incorporated
% ERROR: 5.53
CALIBRATION: 1
OFFSET: 183. M
RAMP: 170.0

MODEL: 2 LAYERS

RESISTIVITY (OHM-M)	THICKNESS (M)	ELEVATION (M)	ELEVATION (FEET)	CONDUCTANCE (S) LAYER	CONDUCTANCE (S) TOTAL
		428.2	1405.0		
9926.62	333.5	-105.2	-345.2	0.1	0.1
2.60					

	TIMES	DATA	CALC	% ERROR	STD ERR
1	2.20E-04	7.09E+03	7.18E+03	-1.178	
2	2.60E-04	5.22E+03	5.18E+03	0.630	
3	3.55E-04	3.75E+03	3.77E+03	-0.512	
4	4.43E-04	2.76E+03	2.81E+03	-1.839	
5	5.64E-04	1.97E+03	2.05E+03	-4.313	
6	7.13E-04	1.45E+03	1.52E+03	-4.271	
7	8.81E-04	1.11E+03	1.16E+03	-4.325	
8	1.10E-03	8.53E+02	8.81E+02	-3.171	
9	1.41E-03	6.51E+02	6.43E+02	1.373	
10	1.80E-03	4.94E+02	4.78E+02	3.279	
11	2.22E-03	4.05E+02	3.69E+02	9.608	
12	2.80E-03	2.95E+02	2.81E+02	5.313	
13	3.55E-03	2.12E+02	2.13E+02	-0.346	
14	4.43E-03	1.62E+02	1.65E+02	-1.389	
15	5.64E-03	1.25E+02	1.25E+02	0.186	
16	7.13E-03	9.91E+01	9.66E+01	2.611	

R: 183. X: 0. Y: 183. DL: 366. REQ: 203. CF: 1.0000
TDHZ ARRAY, 16 DATA POINTS, RAMP: 170.0 MICROSEC, DATA: WAIKS
1031 2222 0005 Z OPR XTL L / 10+1000
Ch.21 = 0.17 Ch.22 = 0.89 Ch.23 = 13 Ch.24 = 13
RMS LOG ERROR: 2.34E-02, ANTILOG YIELDS 5.5321 %
LATE TIME PARAMETERS

* Blackhawk Geosciences, Incorporated *

PARAMETER RESOLUTION MATRIX:
"F" MEANS FIXED PARAMETER
P 1 0.00
F 2 0.00 0.00
T 1 -0.01 0.00 0.50
P 1 F 2 T 1

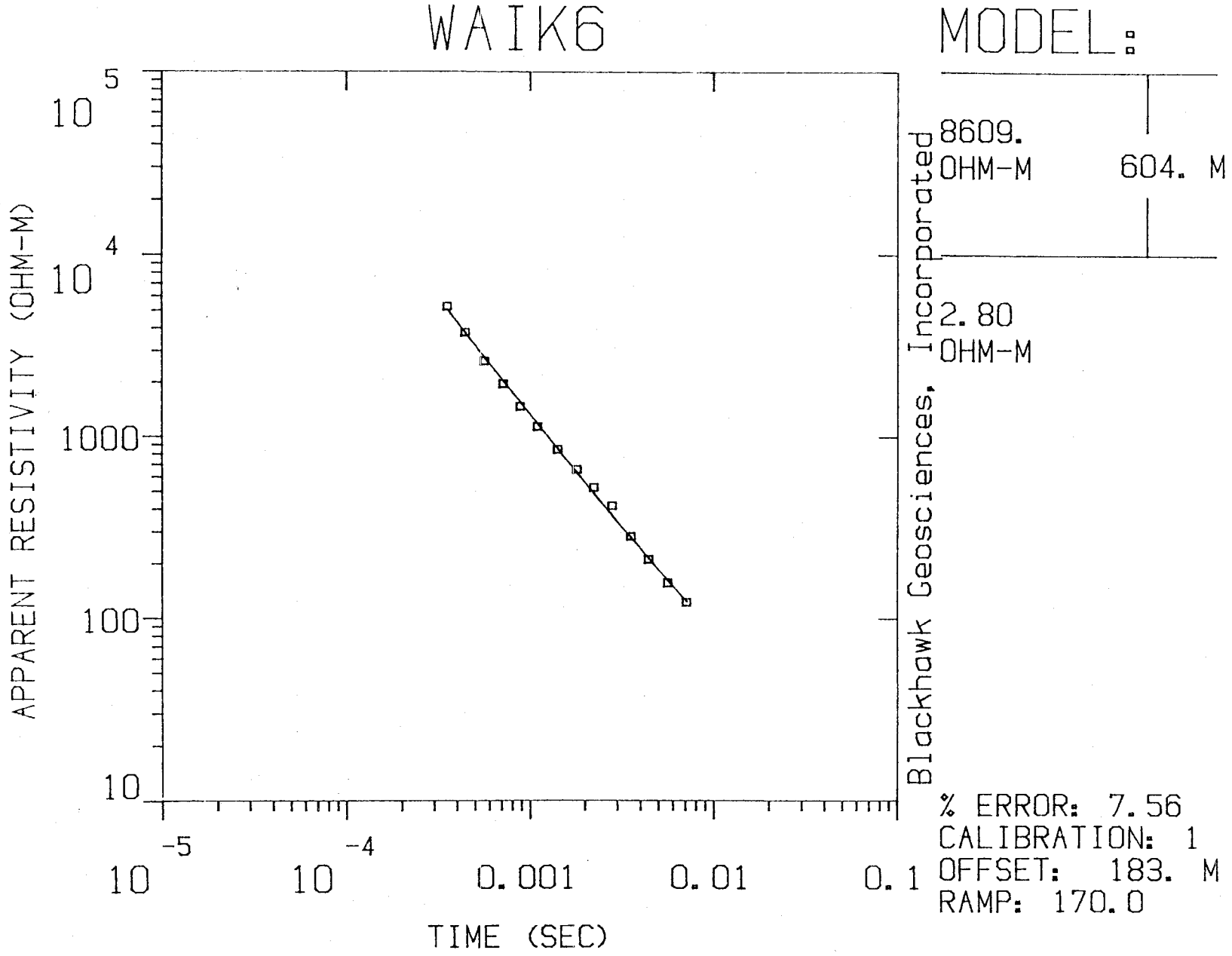
WAIK6
MODEL:
APPARENT RESISTIVITY (OHM-M)
10^5
10^4
1000
100
10
10^-5
10^-4
0.001
0.01
0.1
TIME (SEC)
8609.
OHM-M
604. M
2.80
OHM-M
Blackhawk Geosciences, Incorporated
% ERROR: 7.56
CALIBRATION: 1
OFFSET: 183. M
RAMP: 170.0

MODEL: 2 LAYERS

RESISTIVITY (OHM-M)	THICKNESS (M)	ELEVATION (M)	ELEVATION (FEET)	CONDUCTANCE (S) LAYER	CONDUCTANCE (S) TOTAL
		470.5	1560.0		
3609.00	604.3	-128.3	-422.5	0.1	0.1
2.80					

	TIMES	DATA	CALC	% ERROR	STD ERR
1	3.55E-04	5.23E+03	5.07E+03	3.178	
2	4.43E-04	3.77E+03	3.78E+03	-0.290	
3	5.64E-04	2.61E+03	2.73E+03	-5.043	
4	7.13E-04	1.95E+03	2.04E+03	-4.146	
5	8.81E-04	1.46E+03	1.55E+03	-5.663	
6	1.10E-03	1.13E+03	1.17E+03	-3.808	
7	1.41E-03	8.43E+02	8.56E+02	-0.922	
8	1.80E-03	6.08E+02	6.34E+02	3.826	
9	2.22E-03	5.25E+02	4.86E+02	7.605	
10	2.80E-03	4.13E+02	3.69E+02	12.571	
11	3.55E-03	2.81E+02	2.78E+02	1.282	
12	4.43E-03	2.10E+02	2.14E+02	-2.166	
13	5.64E-03	1.56E+02	1.62E+02	-3.240	
14	7.13E-03	1.22E+02	1.24E+02	-1.049	

R: 183. X: 0. Y: 183. DL: 366. REQ: 203. CF: 1.0000
TDHZ ARRAY, 14 DATA POINTS, RAMP: 170.0 MICROSEC, DATA: MAIN6
1031 2222 0006 Z OPR X/L L 7 10+1000
Ch.21 = 0.17 Ch.22 = 0.99 Ch.23 = 13 Ch.24 = 13
RMS LOG ERROR: 3.17E-02, ANTILOG YIELDS 7.5650 %
LATE TIME PARAMETERS

* Blackhawk Geosciences, Incorporated *

PARAMETER RESOLUTION MATRIX:
"F" MEANS FIXED PARAMETER
P 1 0.03
F 2 0.00 0.00
T 1 0.00 0.00 1.00
P 1 F 2 T 1

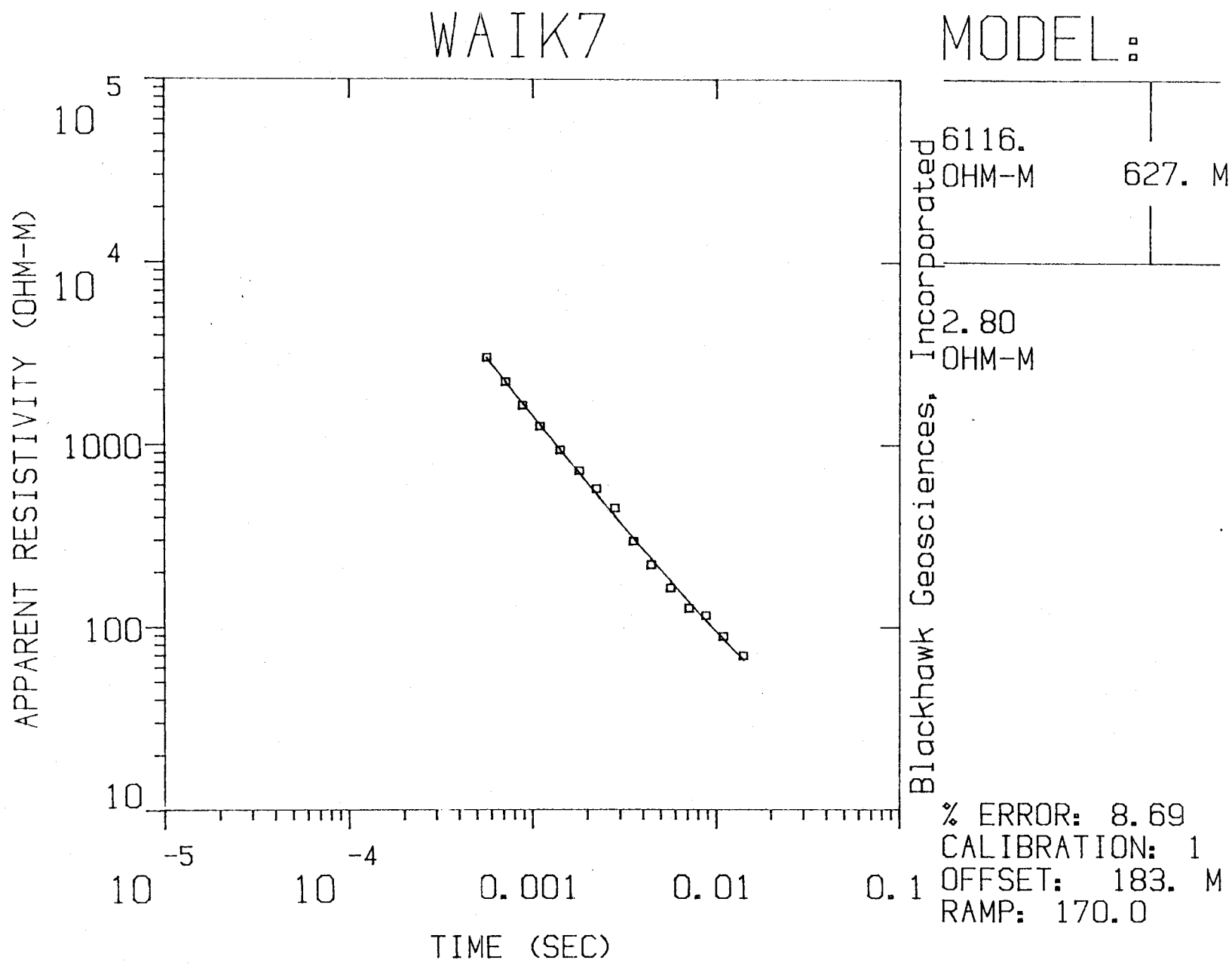
WAIK7
MODEL:
APPARENT RESISTIVITY (OHM-M)
10^5
10^4
1000
100
10
10^-5
10^-4
0.001
0.01
0.1
TIME (SEC)
6116.
OHM-M
627. M
2.80
OHM-M
Blackhawk Geosciences, Incorporated
% ERROR: 8.69
CALIBRATION: 1
OFFSET: 183. M
RAMP: 170.0

MODEL: 2 LAYERS

RESISTIVITY (OHM-M)	THICKNESS (M)	ELEVATION (M)	ELEVATION (FEET)	CONDUCTANCE (S) LAYER	CONDUCTANCE (S) TOTAL
		506.0	1660.0		
6116.43	626.5	-120.5	-395.3	0.1	0.1
2.80					

	TIMES	DATA	CALC	% ERROR	STD ERR
1	5.64E-04	3.01E+03	3.01E+03	0.160	
2	7.13E-04	2.22E+03	2.22E+03	-0.073	
3	8.81E-04	1.64E+03	1.69E+03	-3.030	
4	1.10E-03	1.26E+03	1.29E+03	-2.298	
5	1.41E-03	9.35E+02	9.36E+02	-0.179	
6	1.80E-03	7.16E+02	6.97E+02	2.779	
7	2.22E-03	5.72E+02	5.36E+02	6.805	
8	2.80E-03	4.47E+02	4.03E+02	10.690	
9	3.55E-03	2.95E+02	3.06E+02	-3.715	
10	4.43E-03	2.19E+02	2.36E+02	-7.178	
11	5.64E-03	1.64E+02	1.79E+02	-8.462	
12	7.13E-03	1.27E+02	1.37E+02	-7.552	
13	8.81E-03	1.16E+02	1.09E+02	6.667	
14	1.10E-02	8.89E+01	8.58E+01	3.509	
15	1.41E-02	6.94E+01	6.57E+01	5.692	

R: 183. X: 0. Y: 183. DL: 366. REQ: 203. CF: 1.0000
TOHZ ARRAY, 15 DATA POINTS, RAMP: 170.0 MICROSEC, DATA: WAIK7
1102 0002 0007 Z OPR XTL L 7 10+1000
Ch.21 = 0.17 Ch.22 = 0.89 Ch.23 = 13 Ch.24 = 13
RMS LOG ERROR: 3.62E-02, ANTILOG YIELDS 8.6887 %
LATE TIME PARAMETERS

* Blackhawk Geosciences, Incorporated *

PARAMETER RESOLUTION MATRIX:
"F" MEANS FIXED PARAMETER

P 1	0.03		
F 2	0.00	0.00	
T 1	-0.03	0.00	0.98
	P 1	F 2	T 1

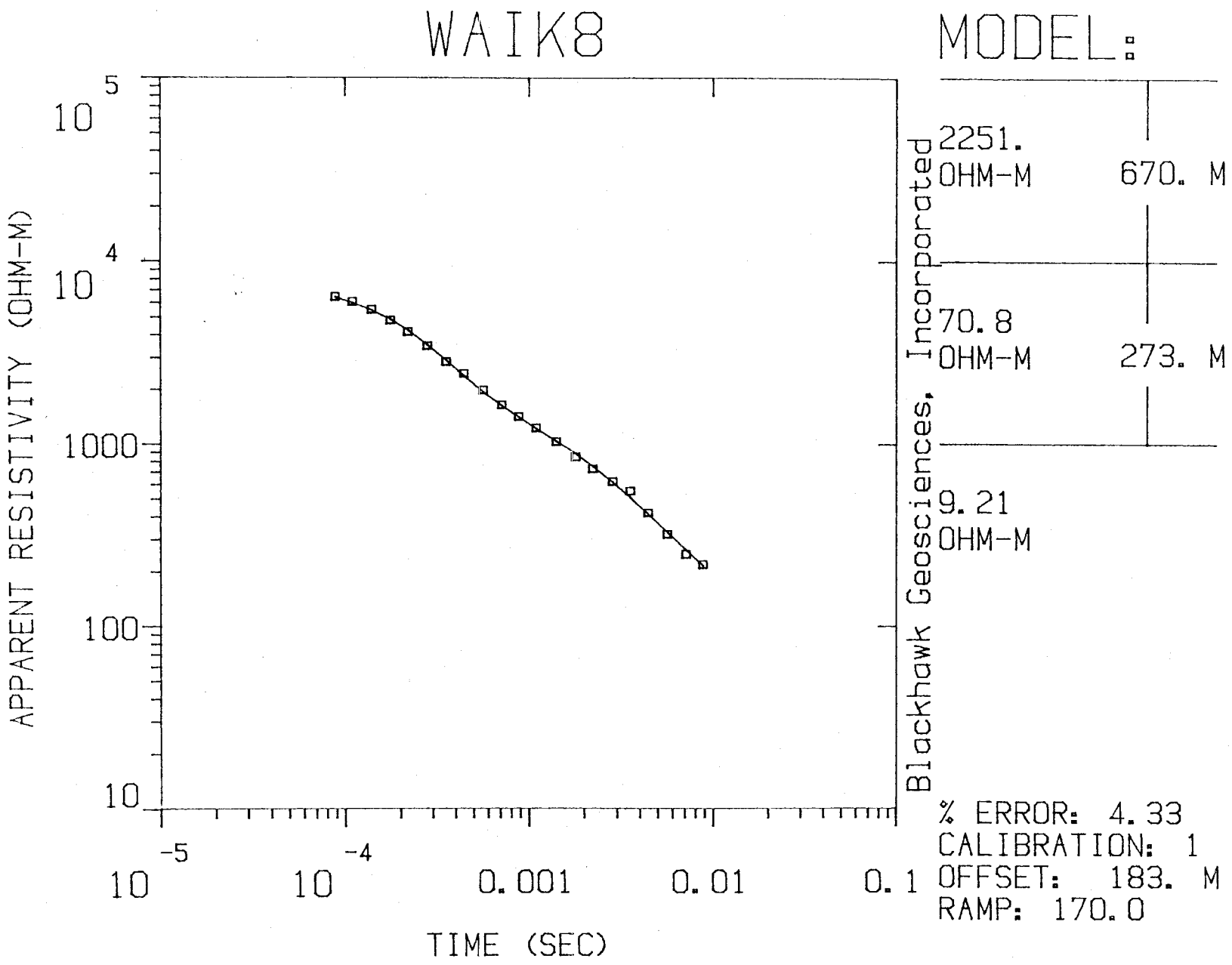
WAIK8
MODEL:
APPARENT RESISTIVITY (OHM-M)
10^5
10^4
1000
100
10
10^-5
10^-4
0.001
0.01
0.1
TIME (SEC)
2251.
OHM-M
670. M
70.8
OHM-M
273. M
9.21
OHM-M
Blackhawk Geosciences, Incorporated
% ERROR: 4.33
CALIBRATION: 1
OFFSET: 183. M
RAMP: 170.0

MODEL: 3 LAYERS

RESISTIVITY (OHM-M)	THICKNESS (M)	ELEVATION (M)	ELEVATION (FEET)	CONDUCTANCE (S) LAYER	CONDUCTANCE (S) TOTAL
		324.3	1720.0		
2250.81	669.8	-145.5	-477.4	0.3	0.3
70.77	272.7	-418.2	-1371.9	3.9	4.2
9.21					

	TIMES	DATA	CALC	% ERROR	STD ERR
1	8.90E-05	6.42E+03	6.41E+03	0.124	
2	1.10E-04	6.04E+03	5.96E+03	1.374	
3	1.40E-04	5.47E+03	5.43E+03	0.790	
4	1.77E-04	4.79E+03	4.85E+03	-1.380	
5	2.20E-04	4.14E+03	4.24E+03	-2.145	
6	2.80E-04	3.47E+03	3.52E+03	-1.532	
7	3.55E-04	2.84E+03	2.89E+03	-1.781	
8	4.43E-04	2.44E+03	2.38E+03	2.717	
9	5.64E-04	1.98E+03	1.93E+03	2.351	
10	7.13E-04	1.64E+03	1.62E+03	0.964	
11	8.81E-04	1.41E+03	1.40E+03	0.589	
12	1.10E-03	1.22E+03	1.21E+03	0.997	
13	1.41E-03	1.03E+03	1.03E+03	-0.409	
14	1.80E-03	8.47E+02	8.86E+02	-4.382	
15	2.22E-03	7.28E+02	7.51E+02	-3.034	
16	2.85E-03	6.21E+02	6.15E+02	0.912	
17	3.55E-03	5.51E+02	5.07E+02	8.563	
18	4.43E-03	4.18E+02	4.12E+02	1.452	
19	5.64E-03	3.20E+02	3.28E+02	-2.459	
20	7.13E-03	2.48E+02	2.62E+02	-5.271	
21	8.81E-03	2.18E+02	2.15E+02	1.677	

R: 183. X: 0. Y: 183. DL: 366. REQ: 203. CF: 1.0000
TOHZ ARRAY, 21 DATA POINTS, RAMP: 170.0 MICROSEC, DATA: WAIK8
1102 0003 0008 Z OPR XTL L 7 10+1000
Ch.21 = 0.17 Ch.22 = 0.89 Ch.23 = 13 Ch.24 = 13
RMS LOG ERROR: 1.84E-02, ANTILOG YIELDS 4.3339 %
LATE TIME PARAMETERS

* Blackhawk Geosciences, Incorporated *

PARAMETER RESOLUTION MATRIX:
"F" MEANS FIXED PARAMETER
P 1 0.11
P 2 -0.01 0.02
P 3 0.00 -0.01 0.00
T 1 0.03 -0.03 -0.03 0.44
T 2 -0.01 0.01 0.00 -0.02 0.03

[illegible]		[illegible]	[illegible]	[illegible]
	1	[illegible]	[illegible]	[illegible]
	2	7.148	9.385	11.726
PHASE	1	660.042	669.764	678.938
	2	253.088	272.656	292.777
DEPTH	1	660.042	669.764	678.938
	2	921.907	942.420	963.446

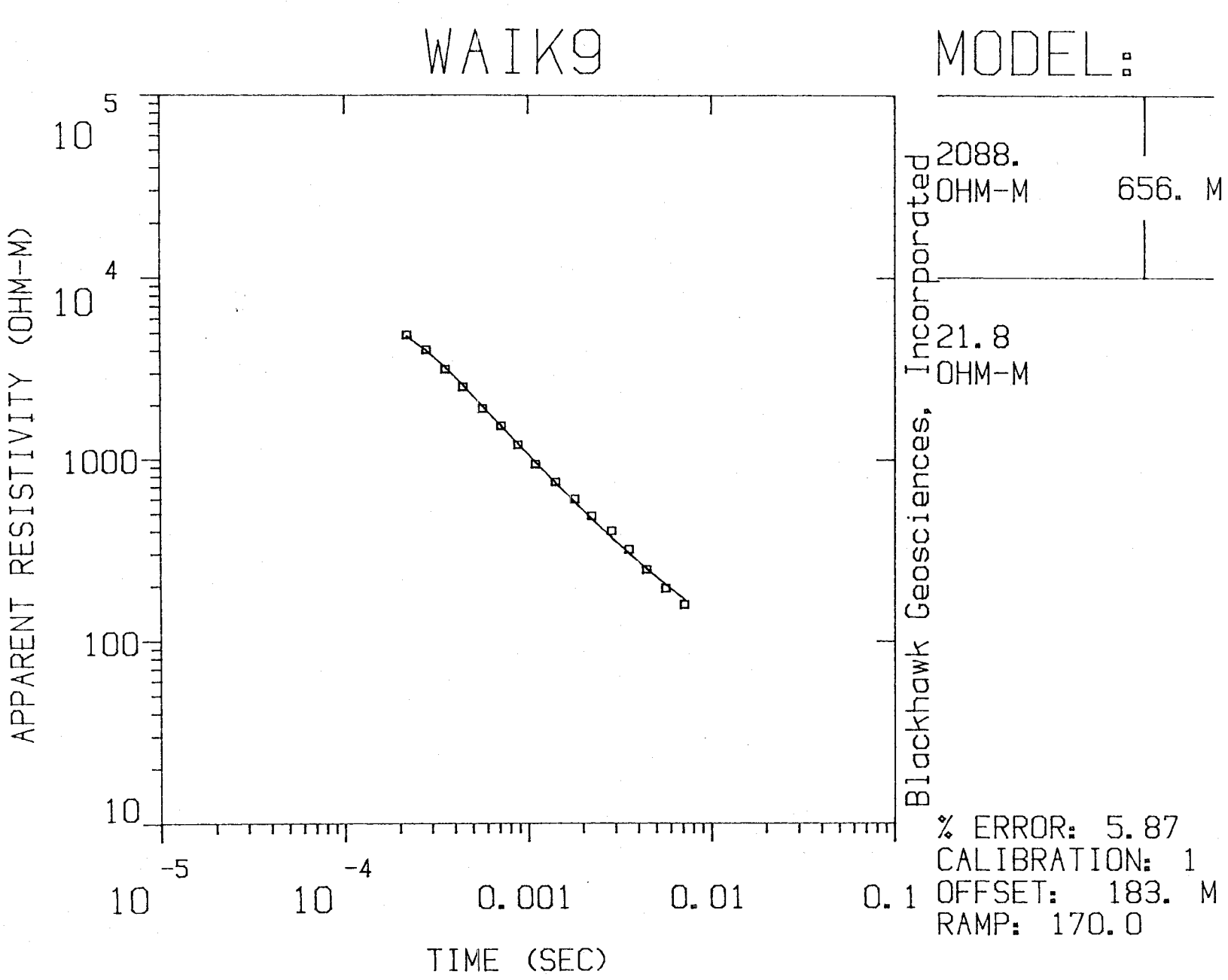
WAIK9
MODEL:
APPARENT RESISTIVITY (OHM-M)
10^5
10^4
1000
100
10
10^-5
10^-4
0.001
0.01
0.1
TIME (SEC)
2088.
OHM-M
656. M
21.8
OHM-M
Blackhawk Geosciences, Incorporated
% ERROR: 5.87
CALIBRATION: 1
OFFSET: 183. M
RAMP: 170.0

MODEL: 2 LAYERS

RESISTIVITY (OHM-M)	THICKNESS (M)	ELEVATION (M)	ELEVATION (FEET)	CONDUCTANCE (S) LAYER	CONDUCTANCE (S) TOTAL
		464.8	1523.0		
2088.39	655.8	-191.0	-626.6	0.3	0.3
21.79					

	TIMES	DATA	CALC	% ERROR	STD ERR
1	2.20E-04	4.87E+03	4.80E+03	1.423	
2	2.86E-04	4.03E+03	4.02E+03	0.663	
3	3.55E-04	3.17E+03	3.26E+03	-2.765	
4	4.43E-04	2.53E+03	2.60E+03	-2.649	
5	5.64E-04	1.92E+03	1.98E+03	-3.157	
6	7.13E-04	1.54E+03	1.54E+03	0.025	
7	8.81E-04	1.20E+03	1.22E+03	-1.617	
8	1.10E-03	9.41E+02	9.67E+02	-2.605	
9	1.41E-03	7.50E+02	7.40E+02	1.341	
10	1.80E-03	6.04E+02	5.81E+02	3.999	
11	2.22E-03	4.87E+02	4.69E+02	3.957	
12	2.80E-03	4.03E+02	3.70E+02	8.923	
13	3.55E-03	3.18E+02	3.03E+02	5.033	
14	4.43E-03	2.46E+02	2.49E+02	-0.926	
15	5.64E-03	1.94E+02	2.04E+02	-4.752	
16	7.13E-03	1.59E+02	1.69E+02	-6.135	

R= 183. X= 0. Y= 183. DL= 366. REQ= 203. CF= 1.0000
TDHZ ARRAY, 16 DATA POINTS, RAMP= 170.0 MICROSEC, DATA: WAIK9
1103 0003 0009 Z OPR XTL L 7 10+1000
Ch.21 = 0.17 Ch.22 = 0.89 Ch.23 = 13 Ch.24 = 13
RMS LOG ERROR: 2.48E-02, ANTILOG YIELDS 5.6733 %
LATE TIME PARAMETERS

* Blackhawk Geosciences, Incorporated *

PARAMETER RESOLUTION MATRIX:
"F" MEANS FIXED PARAMETER
P 1 1.00
P 2 0.00 1.00
T 1 0.00 0.00 1.00
P 1 P 2 T 1

PARAMETER BOUNDS FROM EQUIVALENCE ANALYSIS

	LAYER	MINIMUM	BEST	MAXIMUM
RHO	1	1872.678	7089.394	2417.827
	2	17.213	21.791	27.142
THICK	1	643.211	655.797	668.183

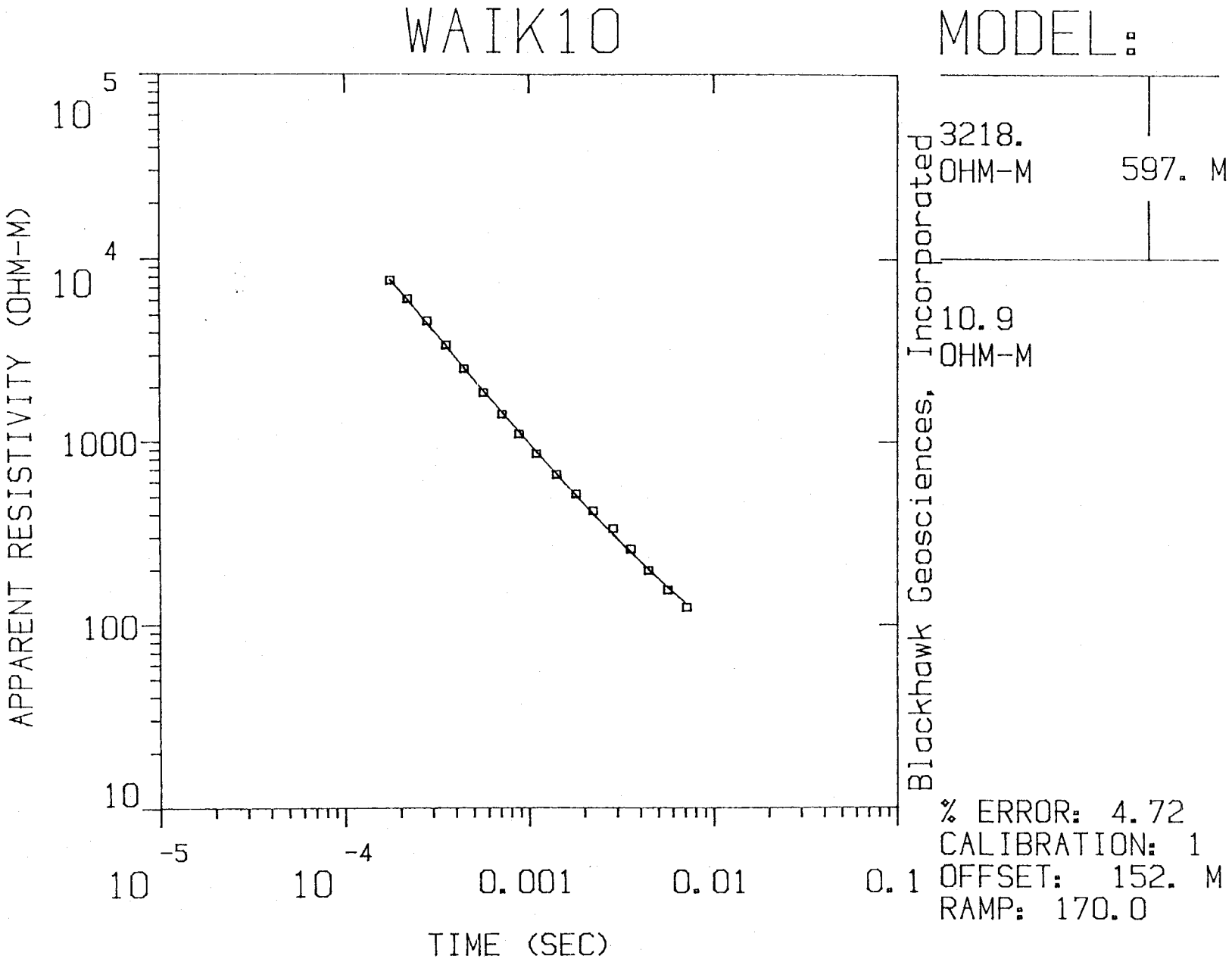
WAIK10
MODEL:
APPARENT RESISTIVITY (OHM-M)
10^5
10^4
1000
100
10
10^-5
10^-4
0.001
0.01
0.1
TIME (SEC)
3218.
OHM-M
597. M
10.9
OHM-M
Blackhawk Geosciences, Incorporated
% ERROR: 4.72
CALIBRATION: 1
OFFSET: 152. M
RAMP: 170.0

INTERVAL VELOCITIES

PROJECTION DISTANCE (KM)	THICKNESS (M)	ELEVATION (M)	ELEVATION (FEET)	LAYER	TOTAL
		426.7	1400.0		
1218.08	597.0	-170.3	-558.7	0.2	0.2
99.4%					

LINES	DATA	CALC	% ERROR	STD ERR
1	1.77E-04	7.07E+03	7.74E+03	-9.55
2	2.20E-04	5.09E+03	4.92E+03	3.11
3	2.80E-04	4.63E+03	4.50E+03	2.79
4	3.55E-04	3.41E+03	3.38E+03	0.85
5	4.43E-04	2.34E+03	2.57E+03	-1.30
6	5.64E-04	1.87E+03	1.92E+03	-2.62
7	7.13E-04	1.41E+03	1.45E+03	-2.77
8	8.81E-04	1.10E+03	1.13E+03	-2.76
9	1.10E-03	8.58E+02	8.78E+02	-2.31
10	1.41E-03	6.09E+02	6.63E+02	-8.47
11	1.80E-03	3.17E+02	3.07E+02	2.98
12	2.22E-03	4.19E+02	4.03E+02	4.04
13	2.85E-03	3.35E+02	3.11E+02	7.66
14	3.50E-03	2.09E+02	2.49E+02	3.90
15	4.43E-03	1.98E+02	2.01E+02	-1.49
16	5.64E-03	1.55E+02	1.60E+02	-3.16
17	7.13E-03	1.25E+02	1.30E+02	-4.16

R: 152. X: 0. Y: 152. DL: 305. RED: 169. CF: 1.0000
TOMZ ARRAY, 17 DATA POINTS, RANF: 170.0 MICROSEC, DATA: MAIN10
1103 0003 0010 2 OMR XTL L 7 10+1000
Ch.21 = 0.155 Ch.22 = 0.89 Ch.23 = 15 Ch.24 = 9
RMS LUG ERROR: 2.00E-02, ANTILOG MISLUS 4.717% %
LATE TIME PARAMETERS

* Blackhawk Geosciences, Incorporated *

PARAMETER RESOLUTION MATRIX:
"F" MEANS FIXED PARAMETER
P 1 0.99
P 2 0.00 0.99
T 1 0.00 0.00 1.00
P 1 P 2 T 1

PARAMETER BOUNDS FROM EQUIVALENCE ANALYSIS

LAYER	THICKNESS	DEPTH	PERCENT
[illegible]	[illegible]	[illegible]	[illegible]